Testing the anomalous color-electric dipole moment of the c quark from $\psi' \to J/\psi + \pi^+ + \pi^-$ at the Beijing Spectrometer

Yu-Ping Kuang,[1,*] Jian-Ping Ma,[2,†] Otto Nachtmann,[3,‡] Wan-Peng Xie,[1,§] and Hui-Huo Zheng[1,4,‖]

[1]*Center for High Energy Physics and Department of Physics, Tsinghua University, Beijing, 100084, China*
[2]*Institute of Theoretical Physics, Academia Sinica, Beijing, 100190, China*
[3]*Institut für Theoretische Physik, Philosophenweg 16, 69120, Heidelberg, Germany*
[4]*Department of Physics, University of Illinois at Urbana-Champaign, 1110 West Green Street, Urbana, Illinois 61801-3080, USA*

(Received 14 February 2012; published 4 June 2012)

If the c quark has an anomalous color-electric dipole moment (CEDM), it may serve as a new source of CP violation. The strength of such a CP violation depends on the size of the CEDM, d_c'. We propose two effective ways of testing it from the large sample of $\psi' \to J/\psi + \pi^+ + \pi^-$ at the Beijing Spectrometer, and the obtained result, $|d_c'| < 3 \times 10^{-14}$ e cm (95% confidence level), gives the first experimentally determined upper bound on the CEDM of the c quark.

DOI: 10.1103/PhysRevD.85.114010 PACS numbers: 14.65.Dw, 13.20.Gd, 13.30.Eg

I. INTRODUCTION

Searching for new sources of CP violation beyond the standard model (SM) is one of the currently interesting projects in particle physics. It concerns the explanation of the asymmetry between matter and antimatter in the Universe. There have been a lot of experimental studies on the CP violation in K-meson, B-meson, and D-meson decays. So far, these experimental results are consistent with the SM predictions [1].

There have been other possible new CP violation sources under consideration, for example, the possible electric dipole moments of quarks or leptons [1]. In Ref. [2], the CP violation effects in Z boson decays were studied. An effective interaction Lagrangian containing the relevant CP-violating terms was presented. These included the electric and weak dipole moments and the color-electric dipole moment (CEDM) of the quarks. In the present paper, we are concerned with the CEDM of the c quark. We note that, to the CP-odd correlations considered in Ref. [2], this CEDM does not contribute. Reference [3] suggested a test via the decay $J/\psi \to \gamma\phi\phi$ based on a naive quark model calculation. Unfortunately, there is no experimental data on the process $J/\psi \to \gamma\phi\phi$ so far. Reference [3] only estimated the testing sensitivity from the statistics. In this paper, we propose a test via the hadronic transition $\psi' \to J/\psi + \pi^+ + \pi^-$ at the Beijing Spectrometer (BES) based on the calculation of QCD multipole expansion [4–7] which has proved to be successful in many processes [7]. BES has accumulated a lot of ψ' decays, and the branching ratio for $\psi' \to J/\psi + \pi + \pi$ is about 50%, which gives a large sample for testing CEDM effect with certain precision providing the first experimental determination of the CEDM of the c quark.

The effective interaction Lagrangian including the CEDM proposed in Ref. [2] is

$$\mathcal{L}_{\mathrm{CEDM}} = -\frac{i}{2} d_c' \bar{\psi}_c \sigma^{\mu\nu} \gamma_5 \frac{\lambda_a}{2} \psi_c G^a_{\mu\nu}, \tag{1}$$

where d_c' is the strength of the CEDM, $\sigma^{\mu\nu} = \frac{i}{2}[\gamma^\mu, \gamma^\nu]$, $\gamma_5 = i\gamma^0\gamma^1\gamma^2\gamma^3$, λ_a is the Gell-Mann matrix for the color $SU(3)_c$ group, and $G^a_{\mu\nu} = \partial_\mu G^a_\nu - \partial_\nu G^a_\mu - g_s f_{abc} G^b_\mu G^c_\nu$ is the field strength of the gluon field.

$\mathcal{L}_{\mathrm{CEDM}}$ affects the hadronic transition processes $\psi' \to J/\psi + \pi^+ + \pi^-$ in two folds:

(i) It contributes to the static potential between c and $\bar{c}$, which causes the mixing between CP-even and CP-odd $c\bar{c}$ bound states, i.e., both ψ' and J/ψ contain certain CP-odd ingredients such as $\psi(^1P_1)$.

(ii) $\mathcal{L}_{\mathrm{CEDM}}$ contributes to the vertices in QCD multipole expansion, so that it affects the transition amplitudes.

In this paper, we shall calculate the above two contributions systematically.

We first treat $\mathcal{L}_{\mathrm{CEDM}}$ as a perturbation to calculate its contribution to the c-$\bar{c}$ static potential with which we calculate the energy shifts and CP violating state mixings.

We then calculate the theoretical prediction for the distribution $d\Gamma(\psi' \to J/\psi + \pi^+ + \pi^-)/dM_{\pi\pi}$ and compare the obtained result with the BES data, which leads to an upper bound of d_c'. Finally we construct a CP-odd operator $\mathcal{O}$ from the initial-state and final-state momenta in $e^+e^- \to \psi' \to J/\psi + \pi^+ + \pi^-$, and calculate its expectation value $\langle\mathcal{O}\rangle$ under the amplitude of $e^+e^- \to \psi' \to J/\psi + \pi^+ + \pi^-$. Since the amplitude contains a CP-odd

*ypkuang@mail.tsinghua.edu.cn
†majp@itp.ac.cn
‡o.nachtmann@thphys.uni-heidelberg.de
§xwp08@mails.tsinghua.edu.cn
‖hzheng8@illinois.edu

piece proportional to d_c', $\langle\mathcal{O}\rangle$ is proportional to d_c'. So measuring $\langle\mathcal{O}\rangle$ can provide another way of testing d_c'. We suggest BESIII to do this measurement.

The CEDM interaction $\mathcal{L}_{\rm CEDM}$ in (1) is a dimension-5 operator in an effective Lagrangian with a scale parameter $\Lambda \sim$ TeV beyond which the SM should be replaced by new physics. The present study is at energies far below Λ and also much below the electroweak symmetry breaking scale. See Ref. [8] for a discussion of the effective Lagrangian approach in such a case. In this paper, we concentrate on studying the contribution of $\mathcal{L}_{\rm CEDM}$ to the hadronic transition $\psi' \to J/\psi\pi\pi$. Here we would like to explain why other higher dimensional CP-odd operators, such as the CP-odd 3-gluonic operator, $\mathcal{O}_G = -(C/6)f_{abc}G^a_{\mu\rho}G^{b\,\rho}_{\nu}G^c_{\lambda\sigma}\epsilon^{\mu\nu\lambda\sigma}$ [9], need not be included in this study. In an effective Lagrangian theory, an operator with dimension $4+n$ is always matched by $1/\Lambda^n$ from its coefficient. Let us first look at the dimension-5 operator $\mathcal{L}_{\rm CEDM}$. Comparing it with the dimension-4 SM quark-gluon interaction, we see that the extra dimension of $\mathcal{L}_{\rm CEDM}$ comes from the extra derivative on the gluon field, i.e., from the gluon momentum k. In the transition $\psi' \to J/\psi\pi\pi$, $k < M_{\psi'} - M_{J/\psi} = 590$ MeV. Thus $\mathcal{L}_{\rm CEDM}$ is suppressed by k/Λ relative to the SM quark-gluon interaction. Next we look at the dimension-6 CP-odd operator O_G. Comparing it with the dimension-4 SM triple-gluon interaction, we see that the two extra dimensions of O_G come from two extra derivatives on 2 gluon fields. Thus O_G is suppressed by k^2/Λ^2 relative to the SM triple-gluon interaction which is of the same order as the SM quark-gluon interaction. So, O_G is suppressed by $k/\Lambda < 5.9 \times 10^{-4}$ relative to $\mathcal{L}_{\rm CEDM}$. There have been many papers estimating the magnitude of the coefficient C in O_G [10,11], and showing that C is really very small. Therefore, theoretically, it is reasonable to take only the leading dimension-5 CP-odd operator $\mathcal{L}_{\rm CEDM}$ into account, and ignore all the higher dimensional CP-odd operators such as O_G in the present study.

This paper is organized as follows. In Sec. II, we calculate the contribution of $\mathcal{L}_{\rm CEDM}$ to the potential between heavy quark and antiquark, and treat it as a perturbation to calculate the energy shifts and state mixings caused by this contribution. We shall see that both J/ψ and ψ' contain the CP-violating ingredient $\psi(1^1P_1)$, etc. These mixed quarkonium states define the initial- and final-state in the transition $\psi' \to J/\psi + \pi^+ + \pi^-$. Then we study the contribution of $\mathcal{L}_{\rm CEDM}$, as a new vertex, to the QCD multipole expansion amplitudes, and calculate all the transition amplitudes up to $O(d_c')$ in Sec. III. In Sec. IV, we calculate the total $M_{\pi\pi}$ distribution $d\Gamma(\psi' \to J/\psi + \pi^+ + \pi^-)/dM_{\pi\pi}$ and compare it with the BES measured result. This leads to an upper bound of d_c' which is the strongest bound obtained so far. In Sec. V, we propose the alternative way of determining d_c' from the experimental data on $\langle\mathcal{O}\rangle$. Section IV is a concluding remark.

II. STATIC POTENTIAL AND STATE MIXING

A. Derivation of the potential

Since d_c' is supposed to be small, the $\mathcal{L}_{\rm CEDM}$ contributions to the potential between c and $\bar{c}$ can be calculated by perturbation similar to the derivation of the Coulomb potential in quantum electrodynamics [12]. Let the conventional heavy quark potential be V_0, and the $\mathcal{L}_{\rm CEDM}$ contributed potential be V_1. The total potential is

$$V = V_0 + V_1. \tag{2}$$

In the following, we take V_0 to be a QCD motivated potential, such as the Cornell potential (the simplest one) [13] or the Chen-Kuang potential (more QCD, and better phenomenological predictions) [14]. Note that the short distance behavior of the Cornell potential is the hardest (steepest) among the QCD motivated potentials, while that of the CK potential is the softest (flattest). Thus comparing the results in the two potential models, we can see the model dependence of the result. Now we calculate V_1 to lowest order perturbation. The Feynman diagrams for the $\mathcal{L}_{\rm CEDM}$ contributions to V_1 are showm in Fig. 1, where the normal vertex is $-ig_s\gamma^\mu(\lambda_a/2)$ for c and $ig_s\gamma^\nu(\lambda_b/2)$ for $\bar{c}$. The shaded circle stands for the CEDM vertex determined by $\mathcal{L}_{\rm CEDM}$.

In the static limit, the obtained V_1 in the momentum representation is

$$V_1(\boldsymbol{q}) = i\frac{4}{3}\frac{g_s d_c'}{2}\frac{(\boldsymbol{\sigma}-\bar{\boldsymbol{\sigma}})\cdot\boldsymbol{q}}{|\boldsymbol{q}|^2 - i\epsilon}. \tag{3}$$

Making the Fourier transformation, we finally obtain

$$V_1(\boldsymbol{r}) = \frac{4g_s}{3}d_c'(\boldsymbol{\sigma}-\bar{\boldsymbol{\sigma}})\cdot\boldsymbol{r}\,\delta^{(3)}(\boldsymbol{r}) - \frac{4}{3}\frac{g_s}{4\pi}d_c'\frac{(\boldsymbol{\sigma}-\bar{\boldsymbol{\sigma}})\cdot\boldsymbol{r}/r}{r^2}. \tag{4}$$

The first term serves as a repulsive core, while the second term is an attractive force. We shall see later, especially

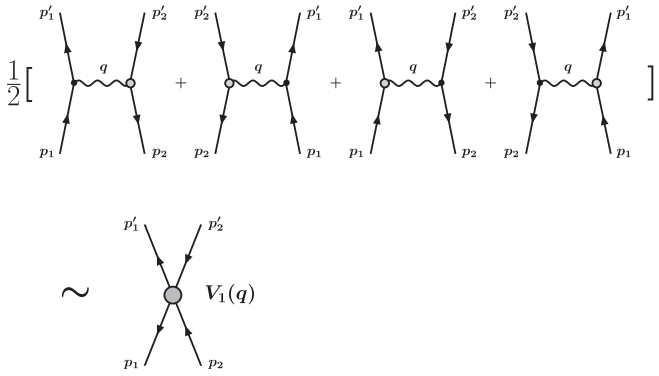

FIG. 1. Lowest order Feynman diagrams for V_1, where • is the normal vertex and the shaded circle is the CEDM vertex.

from Eq. (A10) in the Appendix, that to first order perturbation, the first term does not make any contributions to the energy level and the wave function corrections, so that only the second term matters. Note that the dimension of d_c' is m^{-1}. So it is natrual to define

$$d_c' \equiv \frac{\delta_c}{m_c}, \tag{5}$$

where δ_c is a dimensionless parameter. Then $V_1(\boldsymbol{r})$ can be expressed by

$$V_1(\boldsymbol{r}) = \frac{4g_s}{3}\frac{\delta_c}{m_c}(\boldsymbol{\sigma}-\bar{\boldsymbol{\sigma}})\cdot\boldsymbol{r}\,\delta^{(3)}(\boldsymbol{r}) - \frac{4}{3}\frac{g_s}{4\pi}\frac{\delta_c}{m_c}\frac{(\boldsymbol{\sigma}-\bar{\boldsymbol{\sigma}})\cdot\boldsymbol{r}/r}{r^2}. \tag{6}$$

B. Energy shift and state mixing

We see that $V_1(\boldsymbol{r})$ contains a factor $(\boldsymbol{\sigma}-\bar{\boldsymbol{\sigma}})\cdot\boldsymbol{r}$ which flips the quarkonium spins by $\Delta s = \pm 1$ and the quarkonium orbital angular momentum by $\Delta l = \pm 1$. This does not change the charge conjugation but changes the parity, i.e., it violates CP. Take the $^3S_1$ quarkonium as an example. $V_1(\boldsymbol{r})$ changes this state to $^1P_1$. Thus when the potential contains $V_1(\boldsymbol{r})$, the eigenstate is a mixture of the $^3S_1$ and the $^1P_1$ states. This affects the decays of the heavy quarkonia.

Since δ_c is supposed to be small, we can take $V_1(\boldsymbol{r})$ as a perturbation. Let E^0_{nl} and $|n^{(2s+1)}L_J\rangle_0$ ($s = 0, 1$) be the energy eigenvalue and the wave function of the quarkonium eigenstate with only $V_0(r)$.

To first order of δ_c, the correction to the energy eigenvalue is

$$E_{nl} = E^0_{nl} + {}_0\langle n^{(2s+1)}L_J|V_1|n^{(2s+1)}L_J\rangle_0. \tag{7}$$

We know that $|n^{(2s+1)}L_J\rangle_0$ is a CP eigenstate, and V_1 violates CP. So that the diagonal matrix element in Eq. (7) vanishes. Therefore *there is no energy shift to* $O(\delta_c)$. The energy shift is of $O(\delta_c^2)$.

The first order wave function correction is

$$|n^{(2s+1)}L_J\rangle = |n^{(2s+1)}L_J\rangle_0 + \sum_{n'}\frac{{}_0\langle n'^{(2(s\pm1)+1)}(L\pm1)_J|V_1|n^{(2s+1)}L_J\rangle_0}{E^0_{nl}-E^0_{n',l\pm1}} \times |n'^{(2(s\pm1)+1)}(L\pm1)_J\rangle_0. \tag{8}$$

For example,

$$\begin{aligned}
|1^3S_1\rangle &= |1^3S_1\rangle_0 - \frac{{}_0\langle 1^1P_1|V_1|1^3S_1\rangle_0}{E^0_{1^1P_1}-E^0_{1^3S_1}}|1^1P_1\rangle_0 + \cdots\\
|2^3S_1\rangle &= |2^3S_1\rangle_0 + \frac{{}_0\langle 1^1P_1|V_1|2^3S_1\rangle_0}{E^0_{2^3S_1}-E^0_{1^1P_1}}|1^1P_1\rangle_0 + \cdots\\
|1^1P_1\rangle &= |1^1P_1\rangle_0 + \frac{{}_0\langle 1^3S_1|V_1|1^1P_1\rangle_0}{E^0_{1^1P_1}-E^0_{1^3S_1}}|1^3S_1\rangle_0 - \frac{{}_0\langle 2^3S_1|V_1|1^1P_1\rangle_0}{E^0_{2^3S_1}-E^0_{1^1P_1}}|2^3S_1\rangle_0 - \frac{{}_0\langle 1^3D_1|V_1|1^1P_1\rangle_0}{E^0_{1^3D_1}-E^0_{1^1P_1}}|1^3D_1\rangle_0 + \cdots\\
|1^3D_1\rangle &= |1^3D_1\rangle_0 + \frac{{}_0\langle 1^1P_1|V_1|1^3D_1\rangle_0}{E^0_{1^3D_1}-E^0_{1^1P_1}}\times|1^1P_1\rangle_0 + \cdots.
\end{aligned} \tag{9}$$

Here we see explicitly the mixing of the $^3S_1$ and $^1P_1$ states.

The above expressions for the mixed states are not normalized yet. The normalized states are

$$\begin{aligned}
|1^3S_1\rangle &= C^{10}_{10}|1^3S_1\rangle_0 + C^{11}_{10}|1^1P_1\rangle_0 + \cdots\\
|2^3S_1\rangle &= C^{20}_{20}|2^3S_1\rangle_0 + C^{11}_{20}|1^1P_1\rangle_0 + \cdots\\
|1^1P_1\rangle &= C^{11}_{11}|1^1P_1\rangle_0 + C^{10}_{11}|1^3S_1\rangle_0 + C^{20}_{11}|2^3S_1\rangle_0 + C^{12}_{11}|1^3D_1\rangle_0 + \cdots\\
|1^3D_1\rangle &= C^{12}_{12}|1^3D_1\rangle_0 + C^{11}_{12}|1^1P_1\rangle_0 + \cdots,
\end{aligned} \tag{10}$$

where

$$
\begin{aligned}
C_{10}^{10} &= \frac{1}{\sqrt{1+\left(\frac{{}_0\langle 1^1P_1|V_1|1^3S_1\rangle_0}{E^0_{1^1P_1}-E^0_{1^3S_1}}\right)^2}}, \qquad C_{10}^{11} = -\frac{\frac{{}_0\langle 1^1P_1|V_1|1^3S_1\rangle_0}{E^0_{1^1P_1}-E^0_{1^3S_1}}}{\sqrt{1+\left(\frac{{}_0\langle 1^1P_1|V_1|1^3S_1\rangle_0}{E^0_{1^1P_1}-E^0_{1^3S_1}}\right)^2}}, \qquad C_{20}^{20} = \frac{1}{\sqrt{1+\left(\frac{{}_0\langle 1^1P_1|V_1|2^3S_1\rangle_0}{E^0_{2^3S_1}-E^0_{1^1P_1}}\right)^2}},\\
C_{20}^{11} &= \frac{\frac{{}_0\langle 1^1P_1|V_1|2^3S_1\rangle_0}{E^0_{2^3S_1}-E^0_{1^1P_1}}}{\sqrt{1+\left(\frac{{}_0\langle 1^1P_1|V_1|2^3S_1\rangle_0}{E^0_{2^3S_1}-E^0_{1^1P_1}}\right)^2}}, \qquad C_{11}^{11} = \frac{1}{\sqrt{1+\left(\frac{{}_0\langle 1^1P_1|V_1|1^3S_1\rangle_0}{E^0_{1^3S_1}-E^0_{1^1P_1}}\right)^2+\left(\frac{{}_0\langle 1^1P_1|V_1|2^3S_1\rangle_0}{E^0_{2^3S_1}-E^0_{1^1P_1}}\right)^2+\left(\frac{{}_0\langle 1^1P_1|V_1|1^3D_1\rangle_0}{E^0_{1^3D_1}-E^0_{1^1P_1}}\right)^2}},\\
C_{11}^{10} &= \frac{\frac{{}_0\langle 1^3S_1|V_1|1^1P_1\rangle_0}{E^0_{1^1P_1}-E^0_{1^3S_1}}}{\sqrt{1+\left(\frac{{}_0\langle 1^1P_1|V_1|1^3S_1\rangle_0}{E^0_{1^3S_1}-E^0_{1^1P_1}}\right)^2+\left(\frac{{}_0\langle 1^1P_1|V_1|2^3S_1\rangle_0}{E^0_{2^3S_1}-E^0_{1^1P_1}}\right)^2+\left(\frac{{}_0\langle 1^1P_1|V_1|1^3D_1\rangle_0}{E^0_{1^3D_1}-E^0_{1^1P_1}}\right)^2}},\\
C_{11}^{20} &= -\frac{\frac{{}_0\langle 2^3S_1|V_1|1^1P_1\rangle_0}{E^0_{2^3S_1}-E^0_{1^1P_1}}}{\sqrt{1+\left(\frac{{}_0\langle 1^1P_1|V_1|1^3S_1\rangle_0}{E^0_{1^3S_1}-E^0_{1^1P_1}}\right)^2+\left(\frac{{}_0\langle 1^1P_1|V_1|2^3S_1\rangle_0}{E^0_{2^3S_1}-E^0_{1^1P_1}}\right)^2+\left(\frac{{}_0\langle 1^1P_1|V_1|1^3D_1\rangle_0}{E^0_{1^3D_1}-E^0_{1^1P_1}}\right)^2}},\\
C_{11}^{12} &= -\frac{\frac{{}_0\langle 1^3D_1|V_1|1^1P_1\rangle_0}{E^0_{1^3D_1}-E^0_{1^1P_1}}}{\sqrt{1+\left(\frac{{}_0\langle 1^1P_1|V_1|1^3S_1\rangle_0}{E^0_{1^3S_1}-E^0_{1^1P_1}}\right)^2+\left(\frac{{}_0\langle 1^1P_1|V_1|2^3S_1\rangle_0}{E^0_{2^3S_1}-E^0_{1^1P_1}}\right)^2+\left(\frac{{}_0\langle 1^1P_1|V_1|1^3D_1\rangle_0}{E^0_{1^3D_1}-E^0_{1^1P_1}}\right)^2}},\\
C_{12}^{12} &= \frac{1}{\sqrt{1+\left(\frac{{}_0\langle 1^1P_1|V_1|1^3D_1\rangle_0}{E^0_{1^3D_1}-E^0_{1^1P_1}}\right)^2}}, \qquad C_{12}^{11} = \frac{\frac{{}_0\langle 1^1P_1|V_1|1^3D_1\rangle_0}{E^0_{1^3D_1}-E^0_{1^1P_1}}}{\sqrt{1+\left(\frac{{}_0\langle 1^1P_1|V_1|1^3D_1\rangle_0}{E^0_{1^3D_1}-E^0_{1^1P_1}}\right)^2}}.
\end{aligned}
\tag{11}
$$

The detailed calculation of the matrix element ${}_0\langle 1^1P_1|V_1|n^{(2s+1)}L_1\rangle_0$ is given in the Appendix. Expanding these mixing coefficients up to $O(\delta_c/m_c)$ and with the results given in Eqs. (A15a) and (A15b), we obtain

$$
\begin{aligned}
&C_{10}^{10} = 1 + O(\delta_c^2/m_c^2), \qquad C_{10}^{11}(m_f, m_s) \equiv C_{10}^{11}\delta_{m_f,m_s} = \frac{8}{3\sqrt{3}}\frac{\delta_c}{m_c}\frac{I_{10}^{11}}{M_{1P}-M_{J/\psi}}\delta_{m_f,m_s} + O(\delta_c^2/m_c^2),\\
&C_{20}^{20} = 1 + O(\delta_c^2/m_c^2), \qquad C_{20}^{11}(m_f, m_s) \equiv C_{20}^{11}\delta_{m_f,m_s} = -\frac{8}{3\sqrt{3}}\frac{\delta_c}{m_c}\frac{I_{20}^{11}}{M_{\psi'}-M_{1P}}\delta_{m_f,m_s} + O(\delta_c^2/m_c^2),\\
&C_{11}^{11} = 1 + O(\delta_c^2/m_c^2), \qquad C_{11}^{10}(m_f, m_s) \equiv C_{11}^{10}\delta_{m_f,m_s} = -\frac{8}{3\sqrt{3}}\frac{\delta_c}{m_c}\frac{I_{11}^{10}}{M_{1P}-M_{J/\psi}}\delta_{m_f,m_s} + O(\delta_c^2/m_c^2),\\
&C_{11}^{20} = 1 + O(\delta_c^2/m_c^2), \qquad C_{11}^{12}(m_f, m_i+m_s) \equiv C_{10}^{11}\delta_{m_f,m_i+m_s} = -\frac{8}{3}\sqrt{\frac{2}{3}}\frac{\delta_c}{m_c}\frac{I_{11}^{12}}{M_{1D}-M_{1P}}\delta_{m_f,m_i+m_s} + O(\delta_c^2/m_c^2),\\
&C_{12}^{12} = 1 + O(\delta_c^2/m_c^2), \qquad C_{12}^{11}(m_f, m_i+m_s) \equiv C_{12}^{11}\delta_{m_f,m_i+m_s} = \frac{8}{3}\sqrt{\frac{2}{3}}\frac{\delta_c}{m_c}\frac{I_{12}^{11}}{M_{1D}-M_{1P}}\delta_{m_f,m_i+m_s} + O(\delta_c^2/m_c^2),
\end{aligned}
\tag{12}
$$

where m_i, m_f, m_s stands for the magnetic quantum numbers of the initial-state orbital angular momentum, the final-state orbital angular momentum, and the initial-state spin, respectively. The numerical values of these mixing coefficients can be obtained once a potential model is chosen. In the Chen-Kuang (CK) model [14] and Cornell model [13], the values are given in Table I.

TABLE I. Values of the mixing coefficients $C_{n_I l_I}^{n_F l_F}$ in the CK and Cornell models.

	CK model	Cornell model
C_{10}^{11}	$0.1165\delta_c$	$0.1142\delta_c$
C_{20}^{11}	$-0.07119\delta_c$	$-0.07209\delta_c$
C_{12}^{11}	$0.1597\delta_c$	$0.1669\delta_c$
C_{20}^{10}	$-0.01863\delta_c$	$-0.01824\delta_c$
C_{12}^{10}	$-0.03906\delta_c$	$-0.04091\delta_c$

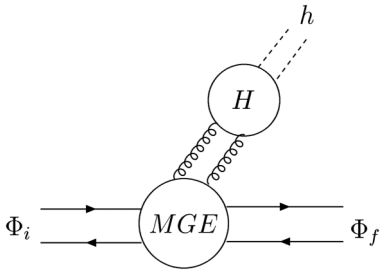

FIG. 2. Diagram for a typical hadronic transition.

Actually, even for $\delta_c = 0$, the states $|2^3S_1\rangle$ and $|1^3D_1\rangle$ are not just the experimentally observed $|\psi'\rangle$ and $|\psi''\rangle$ since the leptonic width of $|1^3D_1\rangle$ is smaller than the experimentally measured value by an order of magnitude. Usually people believe that the observed $|\psi'\rangle$ and $|\psi''\rangle$ are mixtures of $|2^3S_1\rangle$ and $|1^3D_1\rangle$ [15,16]:

$$\begin{aligned} |\psi'\rangle &= |2^3S_1\rangle\cos\theta - |1^3D_1\rangle\sin\theta, \\ |\psi''\rangle &= |2^3S_1\rangle\sin\theta + |1^3D_1\rangle\cos\theta. \end{aligned} \tag{13}$$

The mixing angle θ can be determined by fitting the measured leptonic widths. The obtained values of θ in different models are [15,16]

$$\begin{aligned} \text{Cornell model: } \theta &= 10^\circ, \\ \text{Chen-Kuang model: } \theta &= 12^\circ. \end{aligned} \tag{14}$$

Thus the physical $|\psi'\rangle$ and $|\psi''\rangle$ are [cf. Eq. (10)]

$$\begin{aligned} |\psi'\rangle &= \cos\theta(C_{20}^{20}|2^3S_1\rangle_0 + C_{20}^{11}|1^1P_1\rangle_0) \\ &\quad - \sin\theta(C_{12}^{12}|1^3D_1\rangle_0 + C_{12}^{11}|1^1P_1\rangle_0), \\ |\psi''\rangle &= \sin\theta(C_{20}^{20}|2^3S_1\rangle_0 + C_{20}^{11}|1^1P_1\rangle_0) \\ &\quad + \cos\theta(C_{12}^{12}|1^3D_1\rangle_0 + C_{12}^{11}|1^1P_1\rangle_0). \end{aligned} \tag{15}$$

So the hadronic transition $\psi' \to J/\psi + \pi^+ + \pi^-$ under consideration is expressed as

$$\begin{aligned} &[\cos\theta(C_{20}^{20}|2^3S_1\rangle_0 + C_{20}^{11}|1^1P_1\rangle_0) - \sin\theta(C_{12}^{12}|1^3D_1\rangle_0 \\ &\quad + C_{12}^{11}|1^1P_1\rangle_0)]|_{E=E_{20}} \\ &\to (C_{10}^{10}|1^3S_1\rangle_0 + C_{10}^{11}|1^1P_1\rangle_0)|_{E=E_{10}} + \pi + \pi. \end{aligned} \tag{16}$$

III. CALCULATION OF THE TRANSITION RATES AND DETERMINATION OF THE $O(\delta_c^1)$ SPA COEFFICIENTS

A. $O(\delta_c^0)$ and $O(\delta_c^1)$ transitions

The hadronic transition process is dipicted in Fig. 2, in which the transition amplitude contains two factors, namely, the multipole gluon emission (MGE) factor and the hadronization (H) factor. We shall treat the two factors separately.

We first consider the MGE part. Let $\boldsymbol{E}^a$ and $\boldsymbol{B}^a$ be the color-electric and color-magnetic fields, respectively. In the conventional CP-conserving transitions, the MGE part contains certain quarkonium-gluon interaction vertices, e.g., the color-electric dipole (E1) interaction, the color-magnetic dipole (M1) interaction, etc. [4–6,16]:

$$\begin{aligned} &\text{E1: } -\boldsymbol{d}_a\cdot\boldsymbol{E}^a(\boldsymbol{X},t), \\ &\boldsymbol{d}_a \equiv g_{\rm E}\int(\boldsymbol{x}-\boldsymbol{X})\Psi^\dagger(\boldsymbol{x},t)\frac{\lambda_a}{2}\Psi(\boldsymbol{x},t)d^3x, \\ &\text{M1: } \boldsymbol{m}_a\cdot\boldsymbol{B}^a(\boldsymbol{X},t), \\ &\boldsymbol{m}_a \equiv \frac{g_{\rm M}}{2}\int(\boldsymbol{x}-\boldsymbol{X})\times\Psi^\dagger(\boldsymbol{x},t)\frac{\lambda_a}{2}\gamma^0\boldsymbol{\gamma}\Psi(\boldsymbol{x},t)d^3x, \end{aligned} \tag{17}$$

where $g_{\rm E}$ and $g_{\rm M}$ are effective color-electric and color-magnetic coupling strengths, respectively, $\boldsymbol{X}$ is the center-of-mass coordinate of the quarkonium, and $\Psi(\boldsymbol{x},t)$ is the quarkonium wave function at the space-time point $(\boldsymbol{x},t)$. For the CP-violating CEDM interaction vertex. Equation (1) can be written as

$$\begin{aligned} \mathcal{L}_{\rm CEDM} &= id_c'\psi_c^\dagger\gamma^0\sigma^{0k}\gamma_5\frac{\lambda_a}{2}\psi_c G_{0k}^a \\ &\quad - id_c'\psi_c^\dagger\gamma^0\sigma^{ij}\gamma_5\frac{\lambda_a}{2}\psi_c G_{ij} \\ &= -\frac{\delta_c}{m_c}\psi_c^\dagger\begin{pmatrix}\sigma_i & 0\\ 0 & -\sigma_i\end{pmatrix}\frac{\lambda_a}{2}\psi_c E_i^a \\ &\quad - i\frac{\delta_c}{m_c}\psi_c^\dagger\begin{pmatrix}0 & \sigma_i\\ -\sigma_i & 0\end{pmatrix}\frac{\lambda_a}{2}\psi_c B_i^a. \end{aligned} \tag{18}$$

The first term is just the interaction between the CEDM and the color-electric field. The second term is off diagonal, so that it is nonvanishing only when the lower components of the quark spinor $\pm(\boldsymbol{p}\cdot\boldsymbol{\sigma})/(E+m)$ are taken into account, i.e., when the quark is moving. So the second term means the interaction between the color current and the color-magnetic field. In the

nonrelativistic limit, only the first term is nonvanishing, and the interaction vertex is

$$\text{CEDM}: \ -i\frac{\delta_c}{m_c}\left(\frac{\lambda_a}{2}\boldsymbol{\sigma}+\frac{\bar{\lambda}_a}{2}\bar{\boldsymbol{\sigma}}\right)\cdot\boldsymbol{E}^a. \tag{19}$$

As in the case of M1 transition given in Ref. [4], after certain treatment of the color factor, the effective CEDM vertex is

$$\text{CEDM}: \ -i\frac{\delta_c}{2m_c}(\boldsymbol{\sigma}-\bar{\boldsymbol{\sigma}})\cdot\boldsymbol{E}, \tag{20}$$

where $\boldsymbol{E}\equiv(\lambda_a/2)\boldsymbol{E}^a$.

With these vertices, the transition (16) can be divided into the $O(\delta_c^0)$ terms and $O(\delta_c^1)$ terms. They are:

(i) $O(\delta_c^0)$ *term.*—

(a) Ordinary E1-E1 transition of $2S\to 1S$ with the coefficients $\cos\theta C_{20}^{20}C_{10}^{10}$:

$$\cos\theta C_{20}^{20}|2^3S_1\rangle_0|_{E=E_{20}}\to C_{10}^{10}|1^3S_1\rangle_0|_{E=E_{10}}+\pi+\pi. \tag{21}$$

(b) Ordinary E1-E1 transition of $1D\to 1S$ with the coefficient $-\sin\theta C_{12}^{12}C_{10}^{10}$:

$$-\sin\theta C_{12}^{12}|1^3D_1\rangle_0|_{E=E_{20}}\to C_{10}^{10}|1^3S_1\rangle_0|_{E=E_{10}}+\pi+\pi. \tag{22}$$

(ii) $O(\delta_c^1)$ *terms.*—

(a) Ordinary E1-M1 transition of $2S\to 1P$ with the coefficients $\cos\theta C_{20}^{20}C_{10}^{11}$:

$$\cos\theta C_{20}^{20}|2^3S_1\rangle_0|_{E=E_{20}}\to C_{10}^{11}|1^1P_1\rangle_0|_{E=E_{10}}+\pi+\pi. \tag{23}$$

(b) Ordinary E1-M1 transition of $1D\to 1P$ with the coefficients $-\sin\theta C_{12}^{12}C_{10}^{11}$:

$$-\sin\theta C_{12}^{12}|1^3D_1\rangle_0|_{E=E_{20}}\to C_{10}^{11}|1^1P_1\rangle_0|_{E=E_{10}}+\pi+\pi. \tag{24}$$

(c) Ordinary E1-M1 transition of $1P\to 1S$ with the coefficients $(\cos\theta C_{20}^{11}-\sin\theta C_{12}^{11})$:

$$(\cos\theta C_{20}^{11}-\sin\theta C_{12}^{11})|1^1P_1\rangle_0|_{E=E_{20}}\to C_{10}^{10}|1^3S_1\rangle_0|_{E=E_{10}}+\pi+\pi. \tag{25}$$

(d) M1-CEDM1 transition of $2S\to 1S$ with the coefficients $\cos\theta C_{20}^{20}C_{10}^{10}$:

$$\cos\theta C_{20}^{20}|2^3S_1\rangle_0|_{E=E_{20}}\to C_{10}^{10}|1^3S_1\rangle_0|_{E=E_{10}}+\pi+\pi. \tag{26}$$

(e) E1-CEDM2 transitions of $2S\to 1S$ and $1D\to 1S$ with coefficients $\cos\theta C_{20}^{20}C_{10}^{10}$ and $-\sin\theta C_{12}^{12}C_{10}^{10}$, respectively:

$$\cos\theta C_{20}^{20}|2^3S_1\rangle_0|_{E=E_{20}}\to C_{10}^{10}|1^3S_1\rangle_0|_{E=E_{10}}+\pi+\pi. \tag{27}$$

$$-\sin\theta C_{12}^{12}|1^3D_1\rangle_0|_{E=E_{20}}\to C_{10}^{10}|1^3S_1\rangle_0|_{E=E_{10}}+\pi+\pi. \tag{28}$$

For a given potential model, there is a systematic way of calculating the MGE factors [6,7].

Next we consider the H part, the matrix elements reflecting the conversion of gluons into light hadrons. These matrix elements are at the scale of a few hundred MeV, and the calculation is thus highly nonperturbative. So far, there is no reliable way of calculating them from the first principles of QCD, so that we have to take certain phenomenological approach. A conventionally used approach is the soft-pion approach (SPA) in which the H-factor matrix element is phenomenologically expressed in terms of power expansion of the momenta of the two pions with unknown coefficients [17]. To lowest nonvanishing order, the number of unknown coefficients is usually not large, so that they can be determined from taking certain experimental input data. This approach has proved to be successful in calculating the transition rates, the $M_{\pi\pi}$ distributions, etc. [6,7]. However, in the present case, it will be difficult if we merely take this approach since there are so many kinds of H-factor matrix elements listed in (21)–(28) containing too many unknown coefficients. There are not enough known input experimental data to determine them. Another viable but cruder approach is the two-gluon approach (2GA) proposed and used in Refs. [6,7]. In this approach, the external pion-fields in the H-factor are approximately replaced by two external gluons, so that the matrix elements can be easily evaluated as functions of the pion (gluon) momenta and the two phenomenological coupling constants $g_{\rm E}$ and $g_{\rm M}$ which can be determined by known experimental inputs. Of course this is a crude order of magnitude estimate. However, it has been shown that this crude approach does give right order of magnitudes of transition rates for many processes [6,7,18]. The shortcoming of the 2GA is that it cannot give the correct angular-dependent distributions such as angular distributions, $M_{\pi\pi}$ distributions, etc. This is because that the pion is spinless, while the gluon spin is 1. In this situation, we shall take both SPA and 2GA in this paper for complementarity.

We can first take the 2GA to calculate all the transition rates listed in (21)–(28) which contain two effective coupling constants $g_{\rm E}$ and $g_{\rm M}$. Since the total transition rate $\Gamma(\psi' \to J/\psi\pi\pi)$ is essentially contributed by the $O(\delta_c^0)$ rate which only contains $g_{\rm E}$, we can take the experimental value of $\Gamma(\psi' \to J/\psi\pi\pi)$ [1],

$$\begin{aligned} \Gamma_{\psi'} &= 304 \pm 9 \text{ keV}, \\ B(\psi' \to J/\psi\pi^+\pi^-) &= (33.6 \pm 0.4)\%, \\ B(\psi' \to J/\psi\pi^0\pi^0) &= (17.73 \pm 0.34)\%, \end{aligned} \tag{29}$$

as input to determine $g_{\rm E}$. For the determination of $g_{\rm M}$, we can take the 2GA calculated branching ratio $B(\psi' \to h_c\pi^0) \times B(h_c \to \eta_c\gamma)$ [16] containing $g_{\rm M}/g_{\rm E}$ to compare with the corresponding experimental value [19]. For example, in the CK model and the Cornell model, the determined $g_{\rm E}$ and $g_{\rm M}/g_{\rm E}$ are:

CK model:

$$\alpha_{\rm E} \equiv \frac{g_{\rm E}^2}{4\pi} = 0.523, \qquad \frac{\alpha_{\rm M}}{\alpha_{\rm E}} = \frac{g_{\rm M}^2}{g_{\rm E}^2} = 2.36,$$

Cornell model:

$$\alpha_{\rm E} \equiv \frac{g_{\rm E}^2}{4\pi} = 0.667, \qquad \frac{\alpha_{\rm M}}{\alpha_{\rm E}} = \frac{g_{\rm M}^2}{g_{\rm E}^2} = 2.36. \tag{30}$$

With the determined $g_{\rm E}$ and $g_{\rm M}$, we can obtain all the relative sizes of the transition rates in (21)–(28) with only one undetermined parameter d_c' (or δ_c) left in the $O(\delta_c^1)$ rates. Next, we can take the SPA to calculate all the transition rates containing certain unknown coefficients. As a perturbation calculation, we first obtain the $O(\delta_c^0)$ transition rate containing three unknown coefficients [17] which can be determined by the data (29) and $M_{\pi\pi}$ distribution as what is conventionally done [20]. Then we calculate the $O(\delta_c^1)$ transition rates containing several new unknown coefficients. Comparing the SPA and 2GA results, we can express these unknown coefficients in terms of the known $O(\delta_c^0)$ coefficients, so the SPA results of the $O(\delta_c^1)$ transition amplitudes contain only one undetermined parameter d_c' (or δ_c). We can then calculate the total distribution $d\Gamma(\psi' \to J/\psi + \pi^+ + \pi^-)/dM_{\pi\pi}$ to compare with the BES data for testing d_c' (or δ_c). We shall see that the inclusion of the $O(\delta_C^1)$ contributions does improve the fit, and the best fit value of δ_c is nonvanishing. However, considering the experimental errors, δ_c is still consistent with zero. So we can obtain an upper bound on δ_c (or d_c'). The detailed analysis of this kind of study will be given in Sec. IV.

B. Transition rates of the $O(\delta_c^0)$ processes (21) and (22)

The $O(\delta_c^0)$ transition rates in Eqs. (21) and (22) have been calculated in the published papers [6,7,15]. Here we list the results.

The transitions in (21) and (22) belong to the ordinary E1-E1 transitions. The E1-E1 transition amplitude can be written as [6,7]

$$\begin{aligned} \mathcal{M}_{\rm E1E1} &= i\frac{g_{\rm E}^2}{6}\sum_{KL}\frac{\langle\Phi_F|r_{m_1}|KL\rangle\langle KL|r_{m_2}|\Phi_I\rangle}{E_I - E_{KL}} \\ &\quad\times\langle\pi\pi|E^a_{-m_1}E^a_{-m_2}|0\rangle \\ &= i\frac{g_{\rm E}^2}{6}f^{111}_{n_Il_In_Fl_F}\langle l_Fs_Fj_Fm_F|\hat{r}_{m_1}\hat{r}_{m_2}|l_Is_Ij_Im_I\rangle \\ &\quad\times\langle\pi\pi|E^a_{-m_1}E^a_{m_2}|0\rangle, \end{aligned} \tag{31}$$

where $\Phi_I(\Phi_F)$ is the initial (final) quarkonium state; $\boldsymbol{r}$ is the separation vector between the two heavy quarks; $\hat{r}$ is the unit vector of $\boldsymbol{r}$; $r_{m_1}(r_{m_2})$ is the component of $\boldsymbol{r}$ in the spherical coordinate system with the magnetic quantum number $m_{m_1}(m_{m_2}) \in \{1, 0, -1\}$ [cf. Eq. (A3) in the Appendix]; l, $s.j.m$ are, respectively, the orbital angular momentum, the spin, the total angular momentum, and the total magnetic quantum numbers of the quarkonium state; K (L) is the principal (orbital angular momentum) quantum number of the intermediate state; and E_{KL} is the energy eigenvalue of the intermediate vibrational state $|KL\rangle$. The factor $\langle l_Fs_Fj_Fm_F|\hat{r}_k\hat{r}_l|l_Is_Ij_Im_I\rangle$ can be evaluated using the properties of the spherical harmonics [6], and the reduced amplitude $f^{111}_{n_Il_In_Fl_F}$ is

$$\begin{aligned} &f^{LP_IP_F}_{n_Il_In_Fl_F} \\ &\quad\equiv \sum_K \frac{\int R_F(r)r^{P_F}R^*_{KL}(r)r^2dr\int R^*_{KL}(r')r'^{P_I}R_I(r')r'^2dr'}{M_I - E_{KL}}, \end{aligned} \tag{32}$$

in which R_I, R_F, and R_{KL} are radial wave functions of the initial, final, and intermediate vibrational states, respectively. These radial wave functions are calculated from the Schrödinger equation with a given potential model. The values of various $f^{LP_IP_F}_{n_Il_In_Fl_F}$ in the CK and Cornell models are listed in Table II.

In the following, we consider the approaches to the hadronization factor $\langle\pi\pi|E^a_kE^a_l|0\rangle$.

TABLE II. Values of the reduced amplitudes $f^{LP_IP_F}_{n_Il_In_Fl_F}$ in the CK and Cornell models.

	CK model	Cornell model
f^{111}_{2010} (GeV^{-3})	8.8715	6.9330
f^{000}_{2010} (GeV^{-1})	0.3869	0.3709
f^{111}_{1210} (GeV^{-3})	−11.2507	−8.7701
f^{101}_{1110} (GeV^{-2})	−3.31446	−2.9040
f^{010}_{1110} (GeV^{-2})	−6.8977	−6.1708
f^{110}_{2011} (GeV^{-2})	4.8399	4.2801
f^{001}_{2011} (GeV^{-2})	4.5643	4.0379
f^{110}_{1211} (GeV^{-2})	−5.8859	−5.1934
f^{201}_{1211} (GeV^{-2})	−4.1087	−3.6324

(i) *SPA.*—In the SPA, the hadronization factor can be generally parametrized as [17]

$$\frac{g_E^2}{6}\langle\pi_\alpha(q_1)\pi_\beta(q_2)|E^a_{-m_1}E^a_{-m_2}|0\rangle=\frac{\delta_{\alpha\beta}}{\sqrt{(2\omega_1)(2\omega_2)}}\left\{\delta_{m_1m_2}[\mathcal{A}q_1^\mu q_{2\mu}+\mathcal{B}\omega_1\omega_2]+\mathcal{C}\left(q_{1m_1}q_{2m_2}+q_{1m_2}q_{2m_1}-\frac{2}{3}\delta_{m_1m_2}\boldsymbol{q}_1\cdot\boldsymbol{q}_2\right)\right\}$$
$$=\frac{\mathcal{A}\delta_{\alpha\beta}}{\sqrt{2\omega_1 2\omega_2}}\left\{\delta_{m_1m_2}\left[q_1^\mu q_{2\mu}+\frac{\mathcal{B}}{\mathcal{A}}\omega_1\omega_2\right]+\frac{\mathcal{C}}{\mathcal{A}}\left(q_{1m_1}q_{2m_2}+q_{1m_2}q_{2m_1}-\frac{2}{3}\delta_{m_1m_2}\boldsymbol{q}_1\cdot\boldsymbol{q}_2\right)\right\}, \tag{33}$$

where $\mathcal{A}$, $\mathcal{B}$, and $\mathcal{C}$ are phenomenological constants, and $q_\alpha=(\omega_\alpha,\boldsymbol{q}_\alpha)$ is the four momentum of π_α. For a given invariant mass $M_{\pi\pi}$, the $\mathcal{A}$ term is angular independent, while the $\mathcal{B}$ and $\mathcal{C}$ terms are angular dependent [17].
For $|2^3S_1\rangle\to|1^3S_1\rangle\pi\pi$, the main contributions to the total transition rate are from the $\mathcal{A}$ and $\mathcal{B}$ terms [20], while for $|1^3D_1\rangle\to|1^3S_1\rangle\pi\pi$, the main contribution is from the $\mathcal{C}$ term [6]. Thus the $M_{\pi\pi}$ distribution is [6]

$$\frac{d\Gamma(\psi'\to J/\psi\pi\pi)_{\rm SPA}}{dM_{\pi\pi}}=|\mathcal{A}|^2\left[\cos^2\theta\frac{dG_{\mathcal{AB}}(\psi')}{dM_{\pi\pi}}|f^{111}_{2010}(\psi')|^2+\sin^2\theta\frac{dH_{\mathcal{C}}(\psi')}{dM_{\pi\pi}}|f^{111}_{1210}(\psi')|^2\right]$$
$$=|\mathcal{A}|^2\cos^2\theta\frac{M_{\pi\pi}}{4\pi^3}\frac{M_{J/\psi}}{M_{\psi'}}\left\{\frac{1}{4}(M^2_{\pi\pi}-2m_\pi^2)^2\mathcal{F}_0+\frac{\mathcal{B}}{\mathcal{A}}(M^2_{\pi\pi}-2m_\pi^2)\mathcal{F}_1+\left|\frac{\mathcal{B}}{\mathcal{A}}\right|^2\mathcal{F}_2\right\}|f^{111}_{2010}(\psi')|^2$$
$$+\sin^2\theta\frac{M_{\pi\pi}}{225\pi^3}\frac{M_{J/\psi}}{M_{\psi'}}\left|\frac{\mathcal{C}}{\mathcal{A}}\right|^2\left\{\left[3m_\pi^2(m_\pi^2-K_0^2)+\frac{1}{4}(M^2_{\pi\pi}-2m_\pi^2)^2\right]\mathcal{F}_0\right.$$
$$\left.+(8m_\pi^2-M^2_{\pi\pi})\mathcal{F}_1+4\mathcal{F}_2\right\}|f^{111}_{1210}(\psi')|^2, \tag{34}$$

where

$$\mathcal{F}_0=\frac{|\boldsymbol{K}|}{M_{\pi\pi}}\sqrt{M^2_{\pi\pi}-4m_\pi^2},\qquad \mathcal{F}_1=\mathcal{F}_0\left[\frac{1}{6}\frac{K_0^2}{M^2_{\pi\pi}}(M^2_{\pi\pi}+2m_\pi^2)+\frac{1}{12}(M^2_{\pi\pi}-4m_\pi^2)\right],$$
$$\mathcal{F}_2=\frac{\mathcal{F}_0}{80}\left[\frac{8}{3}\frac{K_0^4}{M^4_{\pi\pi}}(M^4_{\pi\pi}+2M^2_{\pi\pi}m_\pi^2+6m_\pi^4)+\frac{4}{3}\frac{K_0^2}{M^2_{\pi\pi}}(M^2_{\pi\pi}-4m_\pi^2)(M^2_{\pi\pi}+6m_\pi^2)+(M^2_{\pi\pi}-4m_\pi^2)^2\right], \tag{35}$$

in which $(K_0,\boldsymbol{K})$ is the four momentum of the $\pi\pi$ system,

$$|\boldsymbol{K}|\equiv\frac{1}{2M_{\psi'}}\{[(M_{\psi'}+M_{\pi\pi})^2-M^2_{J/\psi}][(M_{\psi'}-M_{\pi\pi})^2-M^2_{J/\psi}]\}^{1/2},\qquad K_0\equiv\frac{1}{M_{\psi'}}(M^2_{\psi'}+M^2_{\pi\pi}-M^2_{J/\psi}). \tag{36}$$

The determination of $\mathcal{A}$, $\mathcal{B}/\mathcal{A}$, and $\mathcal{C}/\mathcal{A}$ will be discussed in Sec. IV.
Integrating over $dM_{\pi\pi}$ in (34), we obtain the transition rate

$$\Gamma(\psi'\to J/\psi\pi\pi)_{\rm SPA}=|\mathcal{A}|^2[\cos^2\theta G_{\mathcal{AB}}(\psi')|f^{111}_{2010}(\psi')|^2+\sin^2\theta H_{\mathcal{C}}(\psi')|f^{111}_{1210}(\psi')|^2], \tag{37}$$

where

$$G_{\mathcal{AB}}\equiv\frac{1}{8\pi^3}\frac{M_{J/\psi}}{M_{\psi'}}\int_{2m_\pi}^{\Delta M}dM^2_{\pi\pi}\left\{\frac{1}{4}(M^2_{\pi\pi}-2m_\pi^2)^2\mathcal{F}_0+\frac{\mathcal{B}}{\mathcal{A}}(M^2_{\pi\pi}-2m_\pi^2)\mathcal{F}_1+\left|\frac{\mathcal{B}}{\mathcal{A}}\right|^2\mathcal{F}_2\right\},$$
$$H_{\mathcal{C}}=\frac{1}{450\pi^3}\frac{M_{J/\psi}}{M_{\psi'}}\int_{2m_\pi}^{\Delta M}dM^2_{\pi\pi}\left|\frac{\mathcal{C}}{\mathcal{A}}\right|^2\left\{\left[3m_\pi^2(m_\pi^2-K_0^2)+\frac{1}{4}(M^2_{\pi\pi}-2m_\pi^2)^2\right]\mathcal{F}_0+(8m_\pi^2-M^2_{\pi\pi})\mathcal{F}_1+4\mathcal{F}_2\right\}, \tag{38}$$

in which $\Delta M\equiv M_{\psi'}-M_{J/\psi}$,
Although this approach can give the reliable $M_{\pi\pi}$ distribution, it cannot be applied to other processes in (21)–(28) since other processes contain new unknown parameters in their hadronization factors, and there are not enough experimental data to determine them. So we have to take the help of the 2GA.

(ii) *2GA.*—The hadronization factor can be further written as

$$\langle\pi\pi|E^a_{-m_1}E^a_{-m_2}|0\rangle = \sum_N \langle\pi\pi|N\rangle\langle N|E^a_{-m_1}E^a_{-m_2}|0\rangle, \tag{39}$$

where $|N\rangle$ denotes a complete set of intermediate states. The 2GA assumes that the color-singlet 2-gluon state $|N\rangle = |g^c g^c\rangle$ dominates. In general, the factor $\langle\pi\pi|g^c g^c\rangle$ is a function of the pion momenta. Considering the fact that the hadronization factors in most hadronic transition processes are all at the few hundred MeV scale, the running of $\langle\pi\pi|g^c g^c\rangle$ with the momentum in such a range of scale is mild. So that we approximately take $\langle\pi\pi|g^c g^c\rangle \approx$ const, and this constant can be absorbed into the redefinition of the effective coupling constant $g_{\rm E}$. Thus we have

$$\langle\pi\pi|E^a_{-m_1}E^a_{-m_2}|0\rangle \approx \langle g^c g^c|E^a_{-m_1}E^a_{-m_2}|0\rangle. \tag{40}$$

This approximation can be extended to other hadronization factors containing color-magnetic field(s). The matrix element $\langle g^c g^c|E^a_{-m_1}E^a_{-m_2}|0\rangle$ can be easily evaluated:

$$\begin{aligned}&\langle g^c g^c|E^a_{-m_1}E^b_{-m_2}|0\rangle \\ &= -\frac{\delta_{ab}}{\sqrt{2\omega_1}\sqrt{2\omega_2}}[\omega_1\epsilon_{1,-m_1}(\lambda_1)\omega_2\epsilon_{2,-m_2}(\lambda_2) \\ &\quad + \omega_1\epsilon_{1,-m_2}(\lambda_1)\omega_2\epsilon_{2,-m_1}(\lambda_2)],\end{aligned} \tag{41}$$

where ω (ω') and $\boldsymbol{\epsilon}$ ($\boldsymbol{\epsilon}'$) are the energy and polarization vector of the gluon, respectively. After lengthy but elementary calculations, we obtain

$$\begin{aligned}&\Gamma_{\rm E1E1}(\psi' \to J/\psi\pi\pi)_{\rm 2GA} \\ &= \left(\frac{g_{\rm E}^2}{6}\right)^2 \frac{8}{27\pi^3}\frac{(\Delta M)^7}{140}\left[\cos^2\theta|f^{111}_{2010}|^2\right. \\ &\quad \left. + \frac{2}{5}\sin^2\theta|f^{111}_{1210}|^2\right].\end{aligned} \tag{42}$$

In the following we shall take the 2GA to calculate other transition rates in (21)–(28), and compare them with (42) to determine their relative sizes.

C. Transition rates of the $O(\delta_c^1)$ E1-M1 processes (23)–(25)

These processes contain δ_c through the mixing coefficients C^{11}_{20}, C^{11}_{10}, and $(\cos\theta C^{11}_{20} - \sin\theta C^{11}_{12})$, respectively [cf. Eqs. (11)]. The transition amplitudes are $|2^3S_1\rangle \to |1^1P_1\rangle + \pi^+ + \pi^-$, $|1^1P_1\rangle \to |1^3S_1\rangle + \pi^+ + \pi^-$, and $|1^3D_1\rangle \to |1^1P_1\rangle + \pi^+ + \pi^-$. They all belong to the ordinary E1-M1 transitions which have been calculated in Refs. [6,16,18]. Here we present the results as follows.

For these three processes, let us denote the initial and final quarkonium states by Φ_I and Φ_F, and the spins of c and $\bar{c}$ by $\boldsymbol{s}_c$ and $\boldsymbol{s}_{\bar{c}}$. Then the E1-M1 transition amplitude can be generally written as

$$\begin{aligned}\mathcal{M}_{\rm E1M1} = i\frac{g_{\rm E}g_{\rm M}}{12m_c}\sum_{KLM_s}&\frac{\langle\Phi_F|r_{m_1}|KLM_s\rangle\langle KLM_s|(s_c - s_{\bar{c}})_{m_2}|\Phi_I\rangle + \langle\Phi_F|(s_c - s_{\bar{c}})_{m_2}|KLM_s\rangle\langle KLM_s|r_{m_1}|\Phi_I\rangle}{M_{\psi'} - E_{KL}} \\ &\times\langle\pi^+\pi^-|E_{-m_1}B_{-m_2}|0\rangle.\end{aligned} \tag{43}$$

Taking the technique of evaluating the spin matrix elements in the MGE factors (cf. the Appendix), and after certain lengthy calculations, we obtain

(a) $|2^3S_1\rangle \to |1^1P_1\rangle + \pi + \pi$.

$$\mathcal{M}_{\rm E1M1}(2^3S_1 \to 1^1P_1\pi\pi) = \frac{\delta_{ab}g_{\rm E}g_{\rm M}}{6\sqrt{3}m_c}(f^{110}_{2011} + f^{001}_{2011})\sum_{m_1m_2}\{a^*_{m_1}(m_F)a_{m_2}(m_I)\}\langle\pi\pi|E_{-m_1}B_{-m_2}|0\rangle, \tag{44}$$

where the definitions of a^* and a are given in Eq. (A5), m_I and m_F are the magnetic quantum numbers of the initial- and final-state, and the definition of $f^{LP_IP_F}_{n_Il_In_Fl_F}$ is given in Eq. (32).

(b) $|1^1P_1\rangle \to |1^3S_1\rangle + \pi + \pi$.

$$\mathcal{M}_{\rm E1M1}(1^1P_1 \to 1^3S_1\pi\pi) = \frac{\delta_{ab}g_{\rm E}g_{\rm M}}{6\sqrt{3}m_c}(f^{010}_{1110} + f^{101}_{1110})\sum_{m_1m_2}\{a^*_{m_1}(m_F)a_{m_2}(m_I)\}\langle\pi\pi|E_{-m_1}B_{-m_2}|0\rangle. \tag{45}$$

and

(c) $|1^3D_1\rangle \to |1^1P_1\rangle + \pi + \pi$.

$$\mathcal{M}_{\rm E1M1}(1^3D_1 \to 1^1P_1\pi\pi) = \frac{\delta_{ab}g_{\rm E}g_{\rm M}}{\sqrt{6}m_c}(f^{110}_{1211} + f^{201}_{1211})\sum_{m_1m_2}\{a^*_{m_1}(m_F)a_{m_2}(m_I)\}\langle\pi\pi|E_{-m_1}B_{-m_2}|0\rangle. \tag{46}$$

Next we take the SPA and 2GA to evaluate the hadronization factor $\langle\pi\pi|E_{-m_1}B_{-m_2}|0\rangle$.

(i) *SPA.*—The hadronization factor $\langle\pi\pi|E_{-m_1}B_{-m_2}|0\rangle$ is a second rank pseudotensor which is to be expressed in terms of the pion momenta in the SPA. To lowest order, the expression is of the form

$$g_{\rm E}g_{\rm M}\langle\pi\pi|E_{-m_1}B_{-m_2}|0\rangle = \mathcal{K}_{\rm E1M1}\epsilon_{-m_1,-m_2,-m_3}\frac{\omega_1 q_{2,m_3}+\omega_2 q_{1,m_3}}{\sqrt{2\omega 2\omega'}}, \tag{47}$$

where $\mathcal{K}_{\rm E1M1}$ is a phenomenological constant. With this expression for the hadronization factor, the amplitudes (44)–(46), after certain evaluation, are

$$\mathcal{M}_{\rm E1M1}(2^3S_1\to 1^1P_1)=\frac{\sqrt{2}\mathcal{K}_{\rm E1M1}\delta_{ab}}{\sqrt{2\omega_1 2\omega_2}}\cos\theta C_{10}^{11}(f_{2011}^{110}+f_{2011}^{001})(-1)^{1+m_f}\begin{pmatrix}1 & 1 & 1\\ m_i+m_s & -m & -m_f\end{pmatrix}(q_1\omega_2+q_2\omega_1)_m, \tag{48}$$

$$\mathcal{M}_{\rm E1M1}(1^1P_1\to 1^3S_1)=-\frac{\sqrt{2}\mathcal{K}_{\rm E1M1}\delta_{ab}}{\sqrt{2\omega_1 2\omega_2}}\sin\theta C_{10}^{11}(f_{1110}^{010}+f_{1110}^{101})(-1)^{m_f+m_s}\begin{pmatrix}1 & 1 & 1\\ m_i & -m & -m_f-m_s\end{pmatrix}(q_1\omega_2+q_2\omega_1)_m, \tag{49}$$

$$\begin{aligned}&\mathcal{M}_{\rm E1M1}(1^3D_1\to 1^1P_1)\\ &=\frac{\mathcal{K}_{\rm E1M1}\delta_{ab}}{\sqrt{2\omega_1 2\omega_2}}(\cos\theta C_{20}^{11}-\sin\theta C_{12}^{11})(f_{2011}^{110}+f_{2011}^{201})(-1)^{1+m_f}\begin{pmatrix}1 & 1 & 1\\ m_i+m_s & -m & -m_f\end{pmatrix}(q_1\omega_2+q_2\omega_1)_m,\end{aligned} \tag{50}$$

where the matrices are the Wigner $3-j$ symbols.
Then, after certain calculations, we get the $M_{\pi\pi}$ distributions

$$\begin{aligned}\frac{d\Gamma_{\rm E1M1}(2^3S_1\to 1^1P_1)_{\rm SPA}}{dM_{\pi\pi}}&=\frac{|\mathcal{K}_{\rm E1M1}|^2}{540\pi^3 m_c^2}|\cos\theta C_{10}^{11}(f_{2011}^{110}+f_{2011}^{001})|^2\frac{M_{J/\psi}}{M_{\psi'}}M_{\pi\pi}\mathcal{F}_0\mathcal{F}_3,\\ \frac{d\Gamma_{\rm E1M1}(1^1P_1\to 1^3S_1)_{\rm SPA}}{dM_{\pi\pi}}&=\frac{|\mathcal{K}_{\rm E1M1}|^2}{540\pi^3 m_c^2}|\sin\theta C_{10}^{11}(f_{1110}^{010}+f_{1110}^{101})|^2\frac{M_{J/\psi}}{M_{\psi'}}M_{\pi\pi}\mathcal{F}_0\mathcal{F}_3,\\ \frac{d\Gamma_{\rm E1M1}(1^3D_1\to 1^1P_1)_{\rm SPA}}{dM_{\pi\pi}}&=\frac{|\mathcal{K}_{\rm E1M1}|^2}{1080\pi^3 m_c^2}|(\cos\theta C_{20}^{11}-\sin\theta C_{12}^{11})(f_{1211}^{110}+f_{1211}^{201})|^2\frac{M_{J/\psi}}{M_{\psi'}}M_{\pi\pi}\mathcal{F}_0\mathcal{F}_3,\end{aligned} \tag{51}$$

where

$$\mathcal{F}_3=(M_{\pi\pi}^2-4m_\pi^2)^2\left[4\frac{K_0^4}{M_{\pi\pi}^4}-3\frac{K_0^2}{M_{\pi\pi}^2}-1\right]+40(M_{\pi\pi}^2-m_\pi^2)m_\pi^2\frac{K_0^2}{M_{\pi\pi}^2}\left(\frac{K_0^2}{M_{\pi\pi}^2}-1\right). \tag{52}$$

Integrating (51) over $dM_{\pi\pi}$, we obtain the transition rates. For example,

$$\Gamma_{\rm E1M1}(2^3S_1\to 1^1P_1)_{\rm SPA}=\frac{|\mathcal{K}_{\rm E1M1}|^2}{540\pi^3}|\cos\theta C_{10}^{11}(f_{2011}^{110}+f_{2011}^{001})|^2\frac{M_{J/\psi}}{M_{\psi'}}\int_{2m_\pi}^{\Delta M}M_{\pi\pi}\mathcal{F}_0\mathcal{F}_3 dM_{\pi\pi}. \tag{53}$$

Now the problem is to determine the unknown constant $\mathcal{K}_{\rm E1M1}$. So far there is no accurate enough data to determine it, so we should take the help of the 2GA.

(ii) *2GA.*—In the 2GA, the hadronization factor can be expressed as

$$\langle\pi\pi|E_{-m_2}B_{-m_1}|0\rangle\approx\langle gg|E_{-m_2}B_{-m_1}|0\rangle=\frac{\omega\epsilon_{-m_2}(\lambda)(\boldsymbol{q}'\times\boldsymbol{\epsilon}'(\lambda'))_{-m_1}+\omega'\epsilon'_{-m_2}(\lambda')(\boldsymbol{q}\times\boldsymbol{\epsilon}(\lambda))_{-m_1}}{\sqrt{2\omega}\sqrt{2\omega'}}. \tag{54}$$

After certain calculations, we obtain

$$\Gamma_{\mathrm{E1M1}}(2^3S_1 \to 1^1P_1\pi\pi)_{\mathrm{2GA}} = \frac{1}{2}\frac{N^2-1}{(2\pi)^5}\left(\frac{g_{\mathrm{E}}g_{\mathrm{M}}}{4Nm_c}\right)^2\frac{128\pi^2}{9}|\cos\theta C_{10}^{11}(f_{2011}^{110}+f_{2011}^{001})|^2\left\{\int_0^{\Delta M}\omega^3(\Delta M-\omega)^3 d\omega\right\}$$
$$= 6\frac{(N^2-1)}{27\pi^3}\left(\frac{g_{\mathrm{E}}g_{\mathrm{M}}}{4Nm_c}\right)^2|\cos\theta C_{10}^{11}(f_{2011}^{110}+f_{2011}^{001})|^2\frac{(\Delta M)^7}{140}. \tag{55}$$

Compared with Eq. (42), we have the ratio

$$R_{\mathrm{E1M1}}^{\mathrm{2GA}} = \frac{\Gamma_{\mathrm{E1M1}}(2^3S_1\to 1^1P_1\pi\pi)}{\Gamma_{\mathrm{E1E1}}(2^3S_1\to 1^3S_1\pi\pi)}\bigg|_{\mathrm{2GA}} = 6\left(\frac{g_{\mathrm{M}}}{2m_c g_{\mathrm{E}}}\right)^2\frac{|\cos\theta C_{10}^{11}(f_{2011}^{110}+f_{2011}^{001})|^2}{|\cos^2\theta f_{2010}^{111}+\frac{2}{5}\sin^2\theta f_{1210}^{111}|^2}. \tag{56}$$

From (53) and (37) we can get the corresponding ratio

$$R_{\mathrm{E1M1}}^{\mathrm{SPA}} = \frac{\Gamma_{\mathrm{E1M1}}(2^3S_1\to 1^1P_1\pi\pi)}{\Gamma_{\mathrm{E1E1}}(2^3S_1\to 1^3S_1\pi\pi)}\bigg|_{\mathrm{SPA}} = \frac{\frac{|\mathcal{K}_{\mathrm{E1M1}}|^2}{540\pi^3m_c^2}|\cos\theta C_{10}^{11}(f_{2011}^{110}+f_{2011}^{001})|^2\frac{M_{J/\psi}}{M_{\psi'}}\int_{2m_\pi}^{\Delta M}M_{\pi\pi}\mathcal{F}_0\mathcal{F}_3 dM_{\pi\pi}}{|\mathcal{A}|^2[\cos^2\theta G_{\mathcal{AB}}(\psi')|f_{2010}^{111}(\psi')|^2+\sin^2\theta H_{\mathcal{K}}(\psi')|f_{1210}^{111}(\psi')|^2]}. \tag{57}$$

As has been argued [6,18], we expect $R_{\mathrm{E1M1}}^{\mathrm{2GA}} \approx R_{\mathrm{E1M1}}^{\mathrm{SPA}}$. Thus from (56) and (57) we have

$$|\mathcal{K}_{\mathrm{E1M1}}|^2 = \frac{6(\frac{g_{\mathrm{M}}}{2m_c g_{\mathrm{E}}})^2}{|\cos^2\theta f_{2010}^{111}+\frac{2}{5}\sin^2\theta f_{1210}^{111}|^2}\frac{|\mathcal{A}|^2[\cos^2\theta G_{\mathcal{AB}}(\psi')|f_{2010}^{111}(\psi')|^2+\sin^2\theta H_{\mathcal{C}}(\psi')|f_{1210}^{111}(\psi')|^2]}{\frac{1}{540\pi^3}\frac{M_{J/\psi}}{M_{\psi'}}\int_{2m_\pi}^{\Delta M}M_{\pi\pi}\mathcal{F}_0\mathcal{F}_3 dM_{\pi\pi}}. \tag{58}$$

So $|\mathcal{K}_{\mathrm{E1M1}}|^2$ is expressed in terms of $\mathcal{A}$, $\mathcal{B}$, and $\mathcal{C}$ appearing in $G_{\mathcal{AB}}$ and $H_{\mathcal{C}}$ [cf. (38)] which will be determined in Sec. IV.

D. Transition rates of the $O(\delta_c^1)$ M1CEDM1 processes (26)

In this transition, δ_c is from the CEDM1 vertex. The transition amplitude is

$$\mathcal{M}_{\mathrm{M1cEDM1}} = \frac{g_{\mathrm{M}}\delta_c}{24m_c^2}\delta_{ab}\sum_{KLM_s}\frac{1}{M_{\psi'}-E_{KL}}\{\langle\Phi_F|(s_c-s_{\bar c})_{m_2}|KLM_s\rangle\langle KLM_s|(s_c-s_{\bar c})_{m_1}|\Phi_I\rangle$$
$$+\langle\Phi_F|(s_c-s_{\bar c})_{m_1}|KLM_s\rangle\langle KLM_s|(s_c-s_{\bar c})_{m_2}|\Phi_I\rangle\}\langle\pi\pi|E_{-m_2}B_{-m_1}|0\rangle$$
$$= \frac{g_{\mathrm{M}}\delta_c}{6m_c^2}\delta_{ab}f_{2010}^{000}\{a_{m_2}(m_f)a_{m_1}^*(m_i)+a_{m_1}(m_f)a_{m_2}^*(m_i)\}\langle\pi\pi|E_{-m_2}B_{-m_1}|0\rangle. \tag{59}$$

The last step is obtained after certain evaluations of the MGE factor.

(i) *SPA.*—In (59), the hadronization factor is the same as in the E1-M1 transition. If we take the lowest order SPA expression (47), we see that it is antisymmetric in m_1 and m_2. However, the MGE factor in (59) is now symmetric in m_1 and m_2, so that the lowest order SPA does not contribute to (59). In this case, we should consider the next term in the SPA for the hadronization factor in (59), i.e., the $O(q^3)$ term. Considering that $\langle\pi\pi|E_{-m_2}B_{-m_1}|0\rangle$ is a second rank pseudotensor, we have

$$\frac{g_{\mathrm{M}}}{24}\delta_{ab}\langle\pi\pi|E_{-m_2}B_{-m_1}|0\rangle = i\frac{\mathcal{K}_{\mathrm{M1CEDM1}}}{\Delta M\sqrt{2\omega_1 2\omega_2}}[(q_1-q_2)_{-m_1}(\boldsymbol{q}_1\times\boldsymbol{q}_2)_{-m_2}+(q_1-q_2)_{-m_2}(\boldsymbol{q}_1\times\boldsymbol{q}_2)_{-m_1}]$$
$$= i\frac{\mathcal{K}_{\mathrm{M1CEDM1}}}{\Delta M\sqrt{2\omega_1 2\omega_2}}[(q_1-q_2)_{-m_1}\epsilon_{-m_2,-m_3,-m_4}q_{1m_3}q_{2m_4}+(q_1-q_2)_{-m_2}\epsilon_{-m_1,-m_3,-m_4}q_{1m_3}q_{2m_4}]. \tag{60}$$

Here we have put a factor i reflecting $\boldsymbol{\partial}\sim i\boldsymbol{q}$ in the expansion for convenience, and have introduced a scale parameter $\Delta M \equiv M_{\psi'}-M_{J/\psi} = \max(\omega_1+\omega_2)$ for making $\mathcal{K}_{\mathrm{M1CEDM1}}$ dimensionless like other SPA coefficients. This expression is symmetric in m_1 and m_2 respecting the Bose symmetry between the two pions. It gives nonvanishing contribution to (59).

With (60), after certain calculations, we obtain

$$\frac{d\Gamma_{\mathrm{M1CEDM1}}(2^3S_1\to 1^3S_1\pi\pi)_{\mathrm{SPA}}}{dM_{\pi\pi}} = \frac{8|\mathcal{K}_{\mathrm{M1CEDM1}}|^2}{3\pi^3|\Delta M|^2}\frac{\delta_c^2}{m_c^4}\frac{M_{J/\psi}}{M_{\psi'}}|f_{2010}^{000}|^2\mathcal{F}_4, \tag{61}$$

$$\mathcal{F}_4 \equiv M_{\pi\pi}\Big\{-4M_{\pi\pi}^2\mathcal{F}_2 + [K_0^2(M_{\pi\pi}^2+4m_\pi^2) + 2M_{\pi\pi}^2(M_{\pi\pi}^2-4m_\pi^2)]\mathcal{F}_1 - (K_0^2+M_{\pi\pi}^2-4m_\pi^2) \times\Big[\frac{1}{4}M_{\pi\pi}^2(M_{\pi\pi}^2-4m_{\pi\pi}^2)+m_\pi^2K_0^2\Big]\mathcal{F}_0\Big\}. \quad (62)$$

Integrating (61) over $dM_{\pi\pi}$, we obtain the transition rate

$$\Gamma_{\mathrm{M1CEDM1}}(2^3S_1\to 1^3S_1\pi\pi)_{\mathrm{SPA}} = \frac{8|\mathcal{K}_{\mathrm{M1CEDM1}}|^2}{3\pi^3|\Delta M|^2}\frac{\delta_c^2}{m_c^4}\frac{M_{J/\psi}}{M_{\psi'}}|f_{2010}^{000}|^2\int_{2m_\pi}^{\Delta M}\mathcal{F}_4 dM_{\pi\pi}. \quad (63)$$

To determine $\mathcal{K}_{\mathrm{M1CEDM1}}$, we do the calculation with the help of the 2GA.

(ii) *2GA.*—The 2GA expression for $\langle\pi\pi|E_{-m_2}B_{-m_1}|0\rangle$ has already been given in (54). After certain calculations, we have

$$\Gamma_{\mathrm{M1CEDM1}}(2^3S_1\to 1^3S_1\pi\pi)_{\mathrm{2GA}} = \frac{32}{9\pi^3}\Big(\frac{g_{\mathrm{M}}\delta_c}{6m_c^2}\Big)^2|f_{2010}^{000}|^2\frac{(\Delta M)^7}{140}. \quad (64)$$

Compared with Eq. (42), we get the ratio

$$R_{\mathrm{M1CEDM1}}^{\mathrm{2GA}}(2^3S_1\to 1^3S_1\pi\pi) = \frac{\Gamma_{\mathrm{M1CEDM1}}(2^3S_1\to 1^3S_1\pi\pi)}{\Gamma_{\mathrm{E1E1}}(2^3S_1\to 1^3S_1\pi\pi)}\Big|_{\mathrm{2GA}} = 12\frac{g_{\mathrm{M}}^2\delta_c^2}{g_{\mathrm{E}}^4m_c^4}\frac{|f_{2010}^{000}|^2}{|\cos^2\theta f_{2010}^{111}+\frac{2}{5}\sin^2\theta f_{1210}^{111}|^2}. \quad (65)$$

Taking $R_{\mathrm{M1CEDM1}}^{\mathrm{2GA}} \approx R_{\mathrm{M1CEDM1}}^{\mathrm{SPA}}$, we determine

$$|\mathcal{K}_{\mathrm{M1CEDM1}}|^2 = 12\frac{g_{\mathrm{M}}^2}{g_{\mathrm{E}}^4}\frac{|\Delta M|^2|f_{2010}^{000}|^2}{|\cos^2\theta f_{2010}^{111}+\frac{2}{5}\sin^2\theta f_{1210}^{111}|^2}\frac{|\mathcal{A}|^2[\cos^2\theta G_{\mathcal{AB}}(\psi')|f_{2010}^{111}(\psi')|^2+\sin^2\theta H_{\mathcal{K}}(\psi')|f_{1210}^{111}(\psi')|^2]}{\frac{8}{3\pi^3}\frac{M_{J/\psi}}{M_{\psi'}}|f_{2010}^{000}|^2\int_{2m_\pi}^{\Delta M}\mathcal{F}_4 dM_{\pi\pi}}, \quad (66)$$

in which $|\mathcal{K}_{\mathrm{M1CEDM1}}|^2$ is expressed in terms of $\mathcal{A}$, $\mathcal{B}$, and $\mathcal{C}$ appearing in $G_{\mathcal{AB}}$ and $H_{\mathcal{C}}$ [cf. (38)].

E. Transition rates of the $O(\delta_c^1)$ E1-CEDM2 processes (27) and (28)

The two processes (27) and (28) for $2^3S_1\to 1^3S_1\pi\pi$ and $1^3D_1\to 1^3S_1\pi\pi$ belong to the E1-CEDM2 transitions (the definition of CEDM2 is similar to that of M2 in $\eta(\pi)$-transitions [5–7,18]). The transition amplitude is of the form

$$\begin{aligned}\mathcal{M}_{\mathrm{E1CEDM2}} &= \frac{g_{\mathrm{E}}\delta_c}{12m_c}\delta_{ab}\sum_{KLM_s}\frac{1}{M_{\Psi'}-E_{KL}}\{\langle\Phi_F\pi\pi|\boldsymbol{S}\cdot\boldsymbol{E}(\boldsymbol{r}\cdot\boldsymbol{\partial})|KLM_s\rangle\langle KLM_s|\boldsymbol{r}'\cdot\boldsymbol{E}|\Phi_I\rangle \\ &\quad+\langle\Phi_F\pi\pi|\boldsymbol{r}\cdot\boldsymbol{E}|KLM_s\rangle\langle KLM_s|\boldsymbol{S}\cdot\boldsymbol{E}(\boldsymbol{r}'\cdot\boldsymbol{\partial})|\Phi_I\rangle\} \\ &= \frac{g_{\mathrm{E}}\delta_c}{4Nm_c}\delta_{ab}\sum_{KLM_s}\frac{1}{M_{\Psi'}-E_{KL}}\{\langle\Phi_F|S_{m_1}r_{m_3}|KLM_s\rangle\langle KLM_s|r'_{m_2}|\Phi_I\rangle\langle\pi\pi|(\partial_{-m_3}E_{-m_1})E_{-m_2}|0\rangle \\ &\quad+\langle\Phi_F|r_{m_1}|KLM_s\rangle\langle KLM_s|S_{m_2}r'_{m_3}|\Phi_I\rangle\langle\pi\pi|E_{-m_1}\partial_{-m_3}E_{-m_2}|0\rangle\},\end{aligned} \quad (67)$$

where $\boldsymbol{S}$ is the total spin operator of c and $\bar{c}$. The matrix element of $\boldsymbol{S}$ between two quarkonium spin states can be evaluated by using Eq. (A20) in the Appendix.

As before, we express the hadronzation factor in SPA and 2GA, respectively.

(i) *SPA.*—In this kind of transition, the hadronization factor is a third rank tensor. Considering the Bose symmetry between the two pions, its general form in the SPA is

$$\begin{aligned}\frac{g_{\mathrm{E}}}{12}\langle\pi\pi|E_{-m_1}\partial_{-m_3}E_{-m_2}|0\rangle &= \frac{g_{\mathrm{E}}}{12}\langle\pi\pi|(\partial_{-m_3}E_{-m_1})E_{-m_2}|0\rangle \\ &= i\frac{\mathcal{K}_{\mathrm{E1CEDM2}}}{\sqrt{2\omega_1 2\omega_2}}(q_{1,-m_2}q_{2,-m_1}+q_{1,-m_1}q_{2,-m_2})(q_{1,-m_3}+q_{2,-m_3}).\end{aligned} \quad (68)$$

Here we also put a factor i reflecting $\boldsymbol{\partial}\sim i\boldsymbol{q}$ for convenience.

After certain evaluations, we obtain

$$\frac{d\Gamma_{\mathrm{E1CEDM2}}(2^3S_1 \to 1^3S_1\pi\pi)_{\mathrm{SPA}}}{dM_{\pi\pi}} = \frac{8|\mathcal{K}_{\mathrm{E1CEDM2}}|^2}{27\pi^3}\frac{\delta_c^2}{m_c^2}\frac{M_{J/\psi}}{M_{\psi'}}|f_{2010}^{111}|^2[\mathcal{F}_5 + 2\mathcal{F}_6] \tag{69}$$

$$\frac{d\Gamma_{\mathrm{E1CEDM2}}(1^3D_1 \to 1^3S_1\pi\pi)_{\mathrm{SPA}}}{dM_{\pi\pi}} = \frac{8|\mathcal{K}_{\mathrm{E1CEDM2}}|^2}{2700\pi^3}\frac{\delta_c^2}{m_c^2}\frac{M_{J/\psi}}{M_{\psi'}}|f_{1210}^{111}|^2\{18K^2(\mathcal{F}_7 + \mathcal{F}_8) - 13\mathcal{F}_5 + 22\mathcal{F}_6\}, \tag{70}$$

where

$$\begin{aligned}
\mathcal{F}_5 &= M_{\pi\pi}\left\{2K_0^2\mathcal{F}_2 - \left[\frac{M_{\pi\pi}^4}{2} + M_{\pi\pi}^2K_0^2 - 2m_\pi^2K_0^2\right]\mathcal{F}_1 + \left[\frac{1}{4}M_{\pi\pi}^2(M_{\pi\pi}^2 + 4m_\pi^2)K_0^2 - m_\pi^2K_0^4 - \frac{M_{\pi\pi}^4}{2}m_\pi^2\right]\mathcal{F}_0\right\},\\
\mathcal{F}_6 &= M_{\pi\pi}\left\{K_0^2\mathcal{F}_2 - \left[(M_{\pi\pi}^2 - m_\pi^2)K_0^2 - \frac{M_{\pi\pi}^4}{4}\right]\mathcal{F}_1 + \frac{1}{8}M_{\pi\pi}^2(M_{\pi\pi}^2 - 2m_\pi^2)(2K_0^2 - M_{\pi\pi}^2)\mathcal{F}_0\right\}\\
\mathcal{F}_7 &= M_{\pi\pi}\left\{\mathcal{F}_2 - (M_{\pi\pi}^2 - 2m_\pi^2)\mathcal{F}_1 + \frac{1}{4}(M_{\pi\pi}^2 - 2m_\pi^2)^2\mathcal{F}_0\right\}\\
\mathcal{F}_8 &= M_{\pi\pi}\{\mathcal{F}_2 + 2m_\pi^2\mathcal{F}_1 + m_\pi^2(m_\pi^2 - K_0^2)\mathcal{F}_0\}.
\end{aligned} \tag{71}$$

Integrating (69) over $dM_{\pi\pi}$, we obtain the transition rate of $\psi(2^3S_1) \to \psi(1^3S_1)\pi\pi$,

$$\Gamma_{\mathrm{E1CEDM2}}(2^3S_1 \to 1^3S_1\pi\pi)_{\mathrm{SPA}} = \frac{8|\mathcal{K}_{\mathrm{E1CEDM2}}|^2}{27\pi^3}\frac{\delta_c^2}{m_c^2}\frac{M_{J/\psi}}{M_{\psi'}}|f_{2010}^{111}|^2\int_{2m_\pi}^{\Delta M}[\mathcal{F}_5 + 2\mathcal{F}_6]dM_{\pi\pi}. \tag{72}$$

Next, we determine the unknown constant $\mathcal{K}_{\mathrm{E1CEDM2}}$ with the help of the 2GA.

(ii) *2GA.*—In the 2GA

$$\begin{aligned}
\langle\pi\pi|E^a_{-m_1}\partial_{-m_3}E^b_{-m_2}|0\rangle &= \frac{-i\delta_{ab}\omega_1\omega_2}{\sqrt{2\omega_1 2\omega_2}}[\epsilon_{1,-m_2}(\lambda_1)\epsilon_{2,m_1}(\lambda_2)q_{2,-m_3} + \epsilon_{2,-m_2}(\lambda_2)\epsilon_{1,-m_1}(\lambda_1)q_{1,-m_3}],\\
\langle\pi\pi|(\partial_{m_3}E^a_{-m_1})E^b_{-m_2}|0\rangle &= \frac{-i\delta_{ab}\omega_1\omega_2}{\sqrt{2\omega_1 2\omega_2}}[\epsilon_{1,-m_2}(\lambda_1)\epsilon_{2,m_1}(\lambda_2)q_{1,-m_3} + \epsilon_{2,-m_2}(\lambda_2)\epsilon_{1,-m_1}(\lambda_1)q_{2,-m_3}].
\end{aligned} \tag{73}$$

With this, we obtain

$$\Gamma_{\mathrm{E1CEDM2}}(2^3S_1 \to 1^3S_1\pi\pi)_{\mathrm{2GA}} = \left(\frac{g_{\mathrm{E}}}{3}\right)^2\frac{\delta_c^2}{m_c^2}|f_{2010}^{111}|^2\frac{(\Delta M)^9}{5103\pi^3}. \tag{74}$$

Compared with Eq. (42), we have the ratio

$$R^{\mathrm{2GA}}_{\mathrm{E1CEDM2}}(2^3S_1 \to 1^3S_1\pi\pi)_{\mathrm{2GA}} = \frac{\Gamma_{\mathrm{E1CEDM2}}(2^3S_1 \to 1^3S_1\pi\pi)}{\Gamma_{\mathrm{E1E1}}(2^3S_1 \to 1^3S_1\pi\pi)}\bigg|_{\mathrm{2GA}} = \frac{10}{27}\left(\frac{\Delta M}{g_{\mathrm{E}}}\right)^2\frac{\delta_c^2}{m_c^2}\frac{|f_{2010}^{111}|^2}{|\cos^2\theta f_{2010}^{111} + \frac{2}{5}\sin^2\theta f_{1210}^{111}|^2}. \tag{75}$$

Taking $R^{\mathrm{2GA}}_{\mathrm{E1CEDM2}} \approx R^{\mathrm{SPA}}_{\mathrm{E1CEDM2}}$, we have

$$|\mathcal{K}_{\mathrm{E1CEDM2}}|^2 = \frac{5}{4}\left(\frac{\Delta M}{g_{\mathrm{E}}}\right)^2\frac{|f_{2010}^{111}|^2}{|\cos^2\theta f_{2010}^{111} + \frac{2}{5}\sin^2\theta f_{1210}^{111}|^2}\frac{|\mathcal{A}|^2[\cos^2\theta G_{\mathcal{AB}}(\psi')|f_{2010}^{111}(\psi')|^2 + \sin^2\theta H_{\mathcal{K}}(\psi')|f_{1210}^{111}(\psi')|^2]}{\frac{1}{\pi^3}\frac{M_{J/\psi}}{M_{\psi'}}|f_{2010}^{111}|^2\int_{2m_\pi}^{\Delta M}[\mathcal{F}_5 + 2\mathcal{F}_6]dM_{\pi\pi}}. \tag{76}$$

So $\mathcal{K}_{\mathrm{E1CEDM2}}$ is expressed in terms of $\mathcal{A}$, $\mathcal{B}$, and $\mathcal{C}$ appearing in $G_{\mathcal{AB}}$ and $H_{\mathcal{C}}$ [cf. (38)].

Now, in the SPA, we have expressed all the unknown constants $|\mathcal{K}_{\mathrm{E1M1}}|^2$, $|\mathcal{K}_{\mathrm{M1CEDM2}}|^2$, and $|\mathcal{K}_{\mathrm{E1CEDM2}}|^2$ occurring in the $O(\delta_c^1)$ transitions in terms of $\mathcal{A}$, $\mathcal{B}$, and $\mathcal{C}$ in the $O(\delta_c^0)$ transitions. The values of $\mathcal{K}_{\mathrm{E1M1}}$, $\mathcal{K}_{\mathrm{M1CEDM2}}$ and $\mathcal{K}_{\mathrm{E1CEDM2}}$ from the values of $\mathcal{A}$, $\mathcal{B}$ and $\mathcal{C}$ obtained from the best fit of the $O(\delta_c^0)$ contribution to the experimental data are listed in Table III. Therefore, the magnitudes of the $O(\delta_c^1)$ transitions are characterized by only one parameter δ_c.

TABLE III. Values of the SPA hadronization factor coefficients $|\mathcal{K}_{\rm E1M1}|$. $|\mathcal{K}_{\rm M1CEDM1}|$ and $|\mathcal{K}_{\rm E1CEDM2}|$ obtained from the best fit values of $|\mathcal{A}|$, $\mathcal{B}/\mathcal{A}$, and $\mathcal{C}/\mathcal{A}$ in the CK and Cornell models.

	CK model	Cornell model
$\lvert\mathcal{K}_{\rm E1M1}\rvert$	3.289	4.208
$\lvert\mathcal{K}_{\rm M1CEDM1}\rvert$	2.318	2.625
$\lvert\mathcal{K}_{\rm E1CEDM2}\rvert$	0.532	0.602

IV. DETERMINATION OF δ_c FROM THE BESII DATA OF $\psi' \to J/\psi + \pi^+ + \pi^-$

In Sec. III, we calculated the transition rates contributed by the mechanisms (21)–(28) individually, and expressed all the unknown coefficients in the SPA in terms of the parameters $\mathcal{A}$, $\mathcal{B}$, and $\mathcal{C}$. Now we are going to determine the parameters $\mathcal{A}$, $\mathcal{B}$, $\mathcal{C}$, and δ_c from the best fit of the theoretical prediction to the experimental data.

The transition amplitudes are functions of the two pion momenta $\mathbf{q_1}$ and $\mathbf{q_2}$. For two transition amplitudes, if their pion momenta dependence belong to the same representation of the spacial rotation and reflection symmetries, they may have nonvanishing interference term in the $M_{\pi\pi}$ distribution. So that we should take account of such interference terms in calculating the $M_{\pi\pi}$ distribution. Specifically, there are three kinds of interference terms to be considered, namely, (i) *E1M1-CEDM2 interference*, (ii) *CEDM2-M1CEDM1 interference*, and (iii) *interference between the* $2^3S_1 \to 1^3S_1\pi\pi$ *and* $1^3D_1 \to 1^3S_1\pi\pi$ *amplitudes in E1CEDM2.* So we should consider the following total transition amplitude:

$$\begin{aligned}\mathcal{M}_{\rm tot}(\psi' \to J/\psi\pi\pi) =& [\cos\theta C_{20}^{20}C_{10}^{10}\mathcal{M}_{\rm E1E1}(2^3S_1 \to 1^3S_1) - \sin\theta C_{12}^{12}C_{10}^{10}\mathcal{M}_{\rm E1E1}(1^3D_1 \to 1^3S_1)]\\ &+ [\cos\theta C_{20}^{20}C_{10}^{10}\mathcal{M}_{\rm M1CEDM1}(2^3S_1 \to 1^3S_1) + \cos\theta C_{20}^{20}C_{10}^{10}\mathcal{M}_{\rm E1CEDM2}(2^3S_1 \to 1^3S_1)\\ &- \sin\theta C_{12}^{12}C_{10}^{10}\mathcal{M}_{\rm E1CEDM2}(1^3D_1 \to 1^3S_1) + \cos\theta C_{10}^{11}C_{20}^{20}\mathcal{M}_{\rm E1M1}(2^3S_1 \to 1^1P_1)\\ &+ (\cos\theta C_{20}^{11} - \sin\theta C_{12}^{11})C_{10}^{10}\mathcal{M}_{\rm E1M1}(1^1P_1 \to 1^3S_1) - \sin\theta C_{10}^{11}C_{12}^{12}\mathcal{M}_{\rm E1M1}(1^3D_1 \to 1^1P_1)]. \end{aligned} \tag{77}$$

We see from Eqs. (34), (51), (61), (69), and (70) that the CEDM contributions to $d\Gamma(\psi' \to J/\psi\pi\pi)/dM_{\pi\pi}$ are of $O(\delta_c^2)$. So that the mixing coefficients C_{10}^{10}, C_{20}^{20}, and C_{12}^{12} in the first square bracket on the right-hand side of Eq. (77) should be expanded up to their $O(\delta_c^2)$ terms which give the CEDM contributions through the normalization of the mixing coefficients, i.e., we should take

$$\begin{aligned} C_{10}^{10} &= \frac{1}{\sqrt{1+(\frac{{}_0\langle 1^1P_1|V_1|1^3S_1\rangle_0}{E^0_{1^1P_1}-E^0_{1^3S_1}})^2}} = 1-\frac{1}{2}|C_{10}^{11}|^2 + O(\delta_c^4),\\ C_{20}^{20} &= \frac{1}{\sqrt{1+(\frac{{}_0\langle 1^1P_1|V_1|2^3S_1\rangle_0}{E^0_{2^3S_1}-E^0_{1^1P_1}})^2}} = 1-\frac{1}{2}|C_{20}^{11}|^2 + O(\delta_c^4),\\ C_{12}^{12} &= \frac{1}{\sqrt{1+(\frac{{}_0\langle 1^1P_1|V_1|1^3D_1\rangle_0}{E^0_{1^3D_1}-E^0_{1^1P_1}})^2}} = 1-\frac{1}{2}|C_{12}^{11}|^2 + O(\delta_c^4), \end{aligned} \tag{78}$$

in the first square bracket on the right-hand-side of (77).

The contributions to $[d\Gamma(\psi' \to J/\psi\pi\pi)]/(dM_{\pi\pi}]$ from individual mechanisms have been given in Eqs. (34), (51), (61), (69), and (70). Now we consider the contributions from the interference terms. By the same approach as in Sec. III, we obtain

(i) E1M1-E1CEDM2:

$$\begin{aligned}\left.\frac{d\Gamma_{\rm E1M1-E1CEDM2}}{dM_{\pi\pi}}\right|_{\rm SPA} &= \mathcal{K}_{\rm E1M1}\mathcal{K}_{\rm E1CEDM2}S_{\rm E1M1}\left\{\frac{2\sqrt{6}M_{J/\psi}M_{\pi\pi}}{27\pi^3m_c^2M_{\psi'}}\cos\theta f_{2010}^{111}\mathcal{F}_9\right.\\ &\left.+\frac{2\sqrt{3}M_{J/\psi}M_{\pi\pi}}{45\pi^3m_c^2M_{\psi'}}\cos\theta f_{2010}^{111}\mathcal{F}_{10}\right\}, \end{aligned} \tag{79}$$

where

$$\begin{aligned} S_{\rm E1M1} \equiv& \sqrt{2}\cos\theta C_{10}^{11}(f_{2011}^{110}+f_{2011}^{001})\\ &-\sqrt{2}(\cos\theta C_{20}^{11}-\sin\theta C_{12}^{11})(f_{1110}^{101}+f_{1110}^{010})\\ &-\sin\theta C_{10}^{11}(f_{1211}^{110}+f_{1211}^{201}), \end{aligned} \tag{80}$$

$$\begin{aligned}\mathcal{F}_9 \equiv K_0\Big[&4\mathcal{F}_2-(2M_{\pi\pi}^2-4m_\pi^2)\mathcal{F}_1\\ &+\left(\frac{1}{4}M_{\pi\pi}^4-m_\pi^2K_0^2\right)\mathcal{F}_0\Big], \end{aligned} \tag{81}$$

$$\begin{aligned}\mathcal{F}_{10} \equiv \frac{1}{6}K_0\Big[&16\mathcal{F}_2-(11M_{\pi\pi}^2-23m_\pi^2)\mathcal{F}_1\\ &+\left(\frac{7}{4}M_{\pi\pi}^4-3m_\pi^2M_{\pi\pi}^2-m_\pi^2K_0^2\right)\mathcal{F}_0\Big]. \end{aligned} \tag{82}$$

(ii) M1CEDM1-E1CEDM2:

$$\left.\frac{d\Gamma_{\mathrm{M1CEDM1-E1CEDM2}}}{dM_{\pi\pi}}\right|_{\mathrm{SPA}} = \frac{2\sqrt{2}M_{J/\psi}M_{\pi\pi}}{5\pi^3 M_{\psi'}\Delta M}\frac{\delta_c^2}{m_c^3}\mathcal{K}_{\mathrm{M1CEDM1}}\mathcal{K}_{\mathrm{E1CEDM2}} \times \cos\theta\sin\theta f^{000}_{2010}f^{111}_{1210}\mathcal{F}_{11}, \quad (83)$$

where

$$\mathcal{F}_{11} \equiv \frac{1}{3}\Big\{-4M^2_{\pi\pi}\mathcal{F}_2 + [K_0^2(M^2_{\pi\pi}+4m_\pi^2) + 2M^2_{\pi\pi}(M^2_{\pi\pi}-4m_\pi^2)]\mathcal{F}_1 - (K_0^2 + M^2_{\pi\pi} - 4m_\pi^2) \times\left[\frac{1}{4}M^2_{\pi\pi}(M^2_{\pi\pi}-4m_\pi^2) + m_\pi^2K_0^2\right]\mathcal{F}_0\Big\}. \quad (84)$$

(iii) E1CEDM2-E1CEDM2:

$$\left.\frac{d\Gamma_{\mathrm{E1CEDM2-E1CEDM2}}}{dM_{\pi\pi}}\right|_{\mathrm{SPA}} = -\frac{8\sqrt{2}M_{J/\psi}M_{\pi\pi}}{45\pi^3 M_{\psi'}}\frac{\delta_c^2}{m_c^2}|\mathcal{K}_{\mathrm{E1CEDM2}}|^2 \times \cos\theta\sin\theta f^{111}_{2010}f^{111}_{1210}\mathcal{F}_{12}, \quad (85)$$

where

$$\mathcal{F}_{12} \equiv \frac{1}{3}\Big\{-4M^2_{\pi\pi}\mathcal{F}_2 + (K_0^2M^2_{\pi\pi} + 2M^4_{\pi\pi} + 4m_\pi^2K_0^2 - 8m_\pi^2M^2_{\pi\pi})\mathcal{F}_1 - (M^2_{\pi\pi} - 4m_\pi^2 + K_0^2)\left(\frac{M^4_{\pi\pi}}{4} + m^2|K|^2\right)\mathcal{F}_0\Big\}. \quad (86)$$

With all these results, we are ready to determine the unknown parameters by the best fit of the theoretical prediction to the experimental data. We take the BESII data on $\psi' \to J/\psi\pi^+\pi^-$ [21] based on 1.4×10^7 ψ' events. We proceed the determination by taking the CEDM effect as a perturbation. We first take the 0th order $O(\delta_c^0)$ contribution to fit the BESII data. There are three unknown parameters $\mathcal{A}$, $\mathcal{B}$ and $\mathcal{C}$ in the 0th order contribution in which $\mathcal{A}$ is an overall normalization factor irrelevant to the $M_{\pi\pi}$ distribution. It is determined by fitting the total transition rate with the experimental value [1]. The ratios $\mathcal{B}/\mathcal{A}$ and $\mathcal{C}/\mathcal{A}$ do affect the $M_{\pi\pi}$ distribution, and they are determined by the best fit of the theoretical $M_{\pi\pi}$ distribution with the BESII data. The best fit curve in the CK model, as an example, is shown by the red dashed line in Fig 3 together with the BESII data.

The values of $|\mathcal{A}|$ determined from (29) and the values of $\mathcal{B}/\mathcal{A}$ and $\mathcal{C}/\mathcal{A}$ determined from the best fit of the $O(\delta_c^0)$ contribution to the $M_{\pi\pi}$ distribution are:

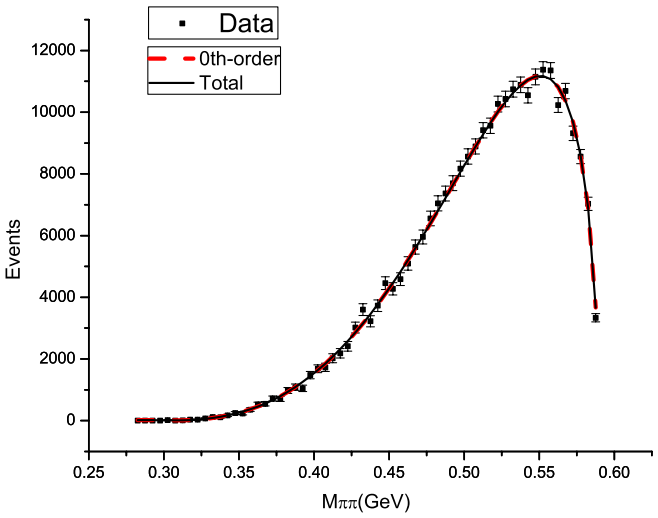

FIG. 3 (color online). The best fit theoretical curves of the 0th order contribution (red dashed line) and the total contribution (dark solid line) in the CK model together with the BESII data on $d\Gamma(\psi' \to J/\psi\pi\pi)/dM_{\pi\pi}$ [21].

$$\begin{aligned} \text{CK Model: } |\mathcal{A}| &= 1.641 \pm 0.036 \\ \mathcal{B}/\mathcal{A} &= -0.372 \pm 0.006, \\ |\mathcal{C}/\mathcal{A}| &= 0.855 \pm 0.020, \\ \text{Cornell model: } |\mathcal{A}| &= 2.09 \pm 0.05 \\ \mathcal{B}/\mathcal{A} &= -0.371 \pm 0.006, \\ |\mathcal{C}/\mathcal{A}| &= 1.000 \pm 0.166. \end{aligned} \quad (87)$$

The values of the SPA coefficients $\mathcal{K}_{\mathrm{E1M1}}$. $\mathcal{K}_{\mathrm{M1CEDM1}}$ and $\mathcal{K}_{\mathrm{E1CEDM2}}$ obtained from the best fit values (87) are listed in Table III.

As an example, we plot the contributions from various $O(\delta_c^2)$ CEDM terms to the $M_{\pi\pi}$ distribution in the CK model in Fig. 4 with $\delta_c = 1$ (the δ_c-independent part). We see that the CEDM contribution increases the low $M_{\pi\pi}$ distribution and reduces the high $M_{\pi\pi}$ distribution, which is just the opposite to the 0th order distribution. This is the reason why the $M_{\pi\pi}$ distribution of $\psi' \to J/\psi\pi^+\pi^-$ can sensitively determine the CEDM parameter δ_c.

Next we take into account the CEDM contributions Eqs. (34), (51), (61), (69), (70), (78), (79), (83), and (85) to make the best fit of the total contribution. The best fit curve of the total contribution is shown by the dark solid line in Fig. 3. The numerical result shows that the dark solid curve improves the fit a little bit (with slightly reduced χ^2 value) although the difference between the two curves is too small to be visible in Fig. 3. The best fit dark solid curve determines the best fit value of δ_c (d_c') listed in Table IV in which the error bars of δ_c (d_c') are determined from the experimental error bars in the $M_{\pi\pi}$ distribution. Note that the best fit value of δ_c is nonvanishing. However, considering the error bars in Table IV, the obtained δ_c is

TABLE IV. The best fit values of δ_c (d_c') in the CK model and the Cornell model.

	CK model		Cornell model	
	68% C.L.	95% C.L.	68% C.L.	95% C.L.
$\lvert\delta_c\rvert$	0.025 ± 0.295	0.025 ± 0.420	0.078 ± 0.373	0.078 ± 0.544
$\lvert d_c'\rvert$ (e. cm)	$(0.110 \pm 1.300) \times 10^{-14}$	$(0.110 \pm 1.851) \times 10^{-14}$	$(0.276 \pm 1.320) \times 10^{-14}$	$(0.276 \pm 1.926) \times 10^{-14}$

still consistent with zero. So the model dependence of the present approach is not serious.

For instance, the 95% confidence level (C.L.) upper bound of d_c' is

$$\begin{aligned} &\text{CK model: } |d_c'| < 1.96 \times 10^{-14}\ \text{e} \cdot \text{cm}, \\ &\text{Cornell model: } |d_c'| < 2.20 \times 10^{-14}\ \text{e} \cdot \text{cm}. \end{aligned} \tag{88}$$

So the model dependence of the present approach is roughly 12%.

We would like to mention that, in Eqs. (58), (66), and (76) , only the absolute values of the SPA coefficients $\mathcal{K}_{\text{E1M1}}$, $\mathcal{K}_{\text{M1CEDM1}}$, and $\mathcal{K}_{\text{E1CEDM2}}$ are determined. So that there is still an uncertain sign in (79) and (83). Actually, If we were able to calculate the hadronization matrix elements from the first principles of QCD, there would not be such sign uncertainties. The present sign uncertainties are due to the phenomenological approach to the haronization factors taken in this paper as lacking of reliable QCD evaluation of the hadronization matrix elements. In Table IV, we only take the simple case that all the SPA coefficients are of the same sign. Now we consider how will the final result affected if they have different signs. First we see from Fig. 4 that the contributions of (83) is so small that its uncertain sign only causes negligible effect in the total $M_{\pi\pi}$ distribution. Thus only the uncertain sign in (79) matters. If we take $\mathcal{K}_{\text{E1M1}}\mathcal{K}_{\text{E1CEDM2}} < 0$ in (79), the total CEDM contribution to $M_{\pi\pi}$ distribution will be reduced, and thus the determined $|\delta_c|$($|d_c'|$) will be larger. Fortunately, we see from Fig. 4 that the E1-M1 CEDM1 contribution is smaller than the individual CEDM contributions. Our calculation shows that the determined $|\delta_c|$ at 68% C.L. will change to 0.047 ± 0.383 for the CK model and 0.123 ± 0.511 for the Cornell model. Then the upper bound of $|d_c'|$ will change to 2.63×10^{-14} e cm for the CK models and 3.09×10^{-14} e cm, i.e., the uncertainty of the upper bound is 34% and 40% for the CK model and the Cornell model, respectively. Therefore the effect of the uncertain signs is not so serious. We conclude that the 95% C.L. upper bound of $|d_c'|$ determined from the BESII data is

$$|d_c'| < 3 \times 10^{-14}\ \text{e cm}. \tag{89}$$

This is the first experimentally determined upper bound of the CEDM of the c quark.

The BES detector has already been updated to BESIII with the efficiency of measuring low momentum pions significantly improved relative to BESII. So far BESIII has accumulated 1.06×10^8 ψ' events, and will be able to accumulate $(7-10) \times 10^8$ ψ' events in 2012. That will be a huge sample. We expect that the new BESIII data may determine δ_c to a higher precision.

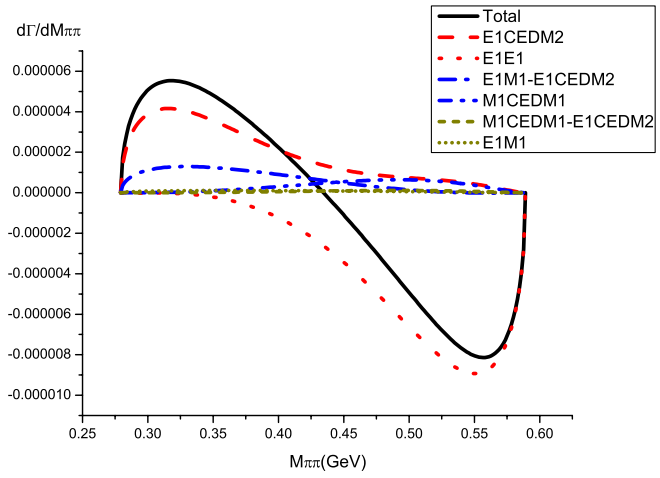

FIG. 4 (color online). Various CEDM contributions to the $M_{\pi\pi}$ distribution for a given δ_c in the CK model.

V. THE *CP*-ODD OPERATOR $\mathcal{O}$

We can propose another way of determining $\delta_c(d_c')$ linearly from the data of $\psi' \to J/\psi\pi\pi$. Consider the process

$$e^+e^- \to \psi' \to J/\psi\pi^+\pi^-. \tag{90}$$

Let $\hat{\boldsymbol{p}}(-\hat{\boldsymbol{p}})$, $\hat{\boldsymbol{q}}_1$, and $\hat{\boldsymbol{q}}_2$ be the unit vectors of the momenta of the positron (electron), π^+, and π^-, respectively. For unpolarized e^+ and e^- in the overall c.m. system, the initial state is then—in the sense of the density matrix—CP-even. Therefore any nonzero expectation value of a CP-odd correlation of the final-state particles is an unambiguous indication of CP violation. With our assumption of the CEDM of the c quark, the expectation values of the CP-odd operators will be linear in $\delta_c(d_c')$. On the other hand, to the expectation values of CP-even operators, the CEDM can only contribute in $O(\delta_c^2)$ or higher even powers. We shall now construct a CP-odd operator for the reaction (90) following Eqs. (3.20) in Ref. [2],

$$\mathcal{O} \equiv \hat{\boldsymbol{p}} \cdot (\hat{\boldsymbol{q}}_1 - \hat{\boldsymbol{q}}_2)\hat{\boldsymbol{p}} \cdot \frac{\hat{\boldsymbol{q}}_1 \times \hat{\boldsymbol{q}}_2}{|\hat{\boldsymbol{q}}_1 \times \hat{\boldsymbol{q}}_2|}. \tag{91}$$

Then we define its expectation value which is an experimental observable:

$$\begin{aligned} \langle\mathcal{O}\rangle &\equiv \frac{1}{N}\int \rho_{M'M}\mathcal{O}d\Gamma_{MM'}(\psi' \to J/\psi\pi\pi), \\ N &\equiv \int \rho_{M'M}d\Gamma_{MM'}(\psi' \to J/\psi\pi\pi), \end{aligned} \tag{92}$$

where $\rho_{M'M}$ is the density matrix, and $M(M')$ stands for the magnetic quantum numbers of ψ'. At the ψ' resonance, the energy of $e^+(e^-)$ is $M_{\psi'}/2$ which is much larger than the electron mass. Thus the colliding $e^+(e^-)$ behaves essentially as a massless fermion. With the standard couplings for the process $e^+e^- \to \gamma^* \to \psi'$, a right-handed e^+ can only annihilate with a left-handed e^- and vice versa. The resulting density matrix for ψ' is

$$\rho_{M'M} = \tfrac{1}{2}(\delta_{M'M} - \delta_{M'0}\delta_{M0}) \qquad M', M \in \{1, 0, -1\}. \tag{93}$$

See Sec. 2.1 in Ref. [2] for the analogous process $e^+e^- \to Z$ and set $g_{Ae} = 0$ there to obtain Eq. (93). In this case the normalization constant N in (92) is just the total transition rate $\Gamma(\psi' \to J/\psi\pi\pi)$ obtained in Sec. IV. Since the CEDM contributions to $\Gamma(\psi' \to J/\psi\pi\pi)$ is negligibly small as can be seen in Fig. 3, we can simply take the 0th order transition rate (37) or even the experimental value $\Gamma(\psi' \to J/\psi\pi\pi) = 156.04 \pm 5.78$ keV [cf. Eq. (29)] for the normalization constant in the following calculation.

Since $\mathcal{O}$ is CP-odd, a nonzero $\langle\mathcal{O}\rangle$ can only be contributed from the CP-odd part of $d\Gamma_{MM'}(\psi' \to J/\psi\pi\pi)$, i.e., the interference terms between the E1E1 transition amplitude and the CEDM transition amplitudes. From the angular part of the phase-space integration, we can see that only the $1^3D_1 \to 1^3S_1\pi\pi$ part in the E1E1 transition gives nonvanishing contribution to the E1E1-E1M1 interference term in (92), while both the $2^3S_1 \to 1^3S_1\pi\pi$ and $1^3D_1 \to 1^3S_1\pi\pi$ parts in the E1E1 transition can give nonvanishing contributions to the E1E1-M1CEDM1 and E1E1-E1CEDM2 interference terms. Thus the result will take the form

$$\langle\mathcal{O}\rangle = \frac{\mathcal{A}}{\Gamma(\psi' \to J/\psi\pi\pi)}\Big\{\mathcal{K}_{\mathrm{M1CEDM1}}\mathcal{I}^{2S\to1S-2S\to1S}_{\mathrm{E1E1-M1CEDM1}} + \mathcal{K}_{\mathrm{E1CEDM2}}\mathcal{I}^{2S\to1S-1D\to1S}_{\mathrm{E1E1-E1CEDM2}} + \frac{\mathcal{C}}{\mathcal{A}}[\mathcal{K}_{\mathrm{E1M1}}\mathcal{I}^{1D\to1S}_{\mathrm{E1E1-E1M1}} + \mathcal{K}_{\mathrm{M1CEDM1}}\mathcal{I}^{1D\to1S-2S\to1S}_{\mathrm{E1E1-M1CEDM1}} + \mathcal{K}_{\mathrm{E1CEDM2}}\mathcal{I}^{1D\to1S-2S\to1S}_{\mathrm{E1E1-E1CEDM2}}]\Big\}\delta_c, \tag{94}$$

where the $\mathcal{I}$'s are the phase-space integrations of the interference terms which can be calculated from the approach similar to those in Sec. IV. So, with the measured value of $\langle\mathcal{O}\rangle$, we can determine δ_c from (94). Our obtained results are:

$$\begin{aligned}
\mathcal{I}^{2S\to1S-2S\to1S}_{\mathrm{E1E1-M1CEDM1}} &= \cos^2\theta\frac{2\delta_c}{15\pi^3m_c^2}\frac{M_{J/\psi}}{\Delta M}f^{111}_{2010}f^{000}_{2010}\int\sin\beta(1-\cos\beta)(q_1q_2^2+q_2q_1^2)\Big(q_1^\mu q_{2\mu}+\frac{\mathcal{B}}{\mathcal{A}}\omega_1\omega_2\Big)d\omega_1d\omega_2,\\
\mathcal{I}^{2S\to1S-1D\to1S}_{\mathrm{E1E1-E1CEDM2}} &= \sin\theta\cos\theta\frac{M_{J/\psi}}{75\sqrt{2}\pi^3}\frac{\delta_c}{m_c}f^{111}_{2010}f^{111}_{1210}\int\sin\beta(1-\cos\beta)(q_1q_2^2+q_1^2q_2)\Big(q_1^\mu q_{2\mu}+\frac{\mathcal{B}}{\mathcal{A}}\omega_1\omega_2\Big)d\omega_1d\omega_2,\\
\mathcal{I}^{1D\to1S}_{\mathrm{E1E1-E1M1}} &= -\sqrt{\frac{3}{2}}\sin\theta\frac{M_{J/\psi}S_{\mathrm{E1M1}}}{900\pi^3m_c}f^{111}_{1210}\int\sin\beta(1-\cos\beta)q_1q_2(\omega_1q_2+\omega_2q_1)d\omega_1d\omega_2,\\
\mathcal{I}^{1D\to1S-2S\to1S}_{\mathrm{E1E1-M1CEDM1}} &= -\sin\theta\cos\theta\frac{\sqrt{2}M_{J/\psi}}{1575\pi^3}\frac{\delta_c}{m_c^3}f^{111}_{1210}f^{000}_{2010}\int\sin\beta(3-2\cos\beta-\cos^2\beta)q_1^2q_2^2(q_1+q_2)d\omega_1d\omega_2,\\
\mathcal{I}^{1D\to1S-2S\to1S}_{\mathrm{E1E1-E1CEDM2}} &= \sin^2\theta\frac{(\sqrt{3}-1)M_{J/\psi}}{2250\pi^3}\frac{\delta_c}{m_c}|f^{111}_{1210}|^2\int\sin^3\beta(q_2^3q_1^2+q_1^3q_2^2)d\omega_1d\omega_2,\\
\cos\beta &\equiv \frac{\boldsymbol{q}_1\cdot\boldsymbol{q}_2}{|\boldsymbol{q}_1||\boldsymbol{q}_2|} = \frac{[M^2_{\psi'}-M^2_{J/\psi}+2m_\pi^2-2M_{\psi'}(\omega_1+\omega_2)+2\omega_1\omega_2]}{2\sqrt{\omega_1^2-m_\pi^2}\sqrt{\omega_2^2-m_\pi^2}},
\end{aligned} \tag{95}$$

where S_{E1M1} is given in (80). The complicated integrations can be carried out numerically, and they lead to the following numerical results in the CK and Cornell models:

$$\begin{aligned}
\text{CK model: } \langle\mathcal{O}\rangle &= \frac{\mathcal{A}}{10^3}\Big\{2.534\mathcal{K}_{\mathrm{M1CEDM1}} - 0.964\mathcal{K}_{\mathrm{E1CEDM2}} + \frac{\mathcal{C}}{\mathcal{A}}[0.0123\mathcal{K}_{\mathrm{E1M1}} + 0.0715\mathcal{K}_{\mathrm{M1CEDM1}} + 0.321\mathcal{K}_{\mathrm{E1CEDM2}}]\Big\}\delta_c,\\
\text{Cornell model: } \langle\mathcal{O}\rangle &= \frac{\mathcal{A}}{10^3}\Big\{1.243\mathcal{K}_{\mathrm{M1CEDM1}} - 0.397\mathcal{K}_{\mathrm{E1CEDM2}} + \frac{\mathcal{C}}{\mathcal{A}}[0.00508\mathcal{K}_{\mathrm{E1M1}} + 0.0290\mathcal{K}_{\mathrm{M1CEDM1}} + 0.321\mathcal{K}_{\mathrm{E1CEDM2}}]\Big\}\delta_c,
\end{aligned} \tag{96}$$

in which the values of $|\mathcal{A}|$ and $|\mathcal{C}/\mathcal{A}|$ in the two models are given in (87), and the values of $\mathcal{K}_{\mathrm{E1M1}}$, $\mathcal{K}_{\mathrm{M1CEDM1}}$, $\mathcal{K}_{\mathrm{E1CEDM2}}$ are given in Table III.

Now we come again to the problem of the uncertain sign similar to those discussed in Sec. IV. We know that, in QCD, there is in principle no sign ambiguity in the various contributions in $\langle\mathcal{O}\rangle$ in (96). But in the present phenomenological approach to the hadronization factors, only the absolute values of the parameters, $|\mathcal{A}|$, $|\mathcal{C}/\mathcal{A}|$, $|\mathcal{K}_{\rm E1M1}|$, $|\mathcal{K}_{\rm M1CEDM1}|$, and $|\mathcal{K}_{\rm E1CEDM2}|$ can be determined as in Sec. III. So, in practice, each of the five parameters has an uncertain sign. The uncertain sign of $\mathcal{A}$ serves as an overall uncertain sign on the right-hand-side (rhs) of (96), which makes us unable to determine the sign of δ_c. Despite of the overall uncertain sign, the values of the curly brackets on the rhs of (96) will be affected by the uncertain signs of $\mathcal{C}/\mathcal{A}$, $\mathcal{K}_{\rm E1M1}$, $\mathcal{K}_{\rm M1CEDM1}$, and $\mathcal{K}_{\rm E1CEDM2}$. The largest term in the curly brackets in (96) is the first term. Without losing generality, we can always take $\mathcal{K}_{\rm M1CEDM1} > 0$ with the uncertain sign of $\mathcal{A}$ taken into account. If we take $\mathcal{C}/\mathcal{A}$, $\mathcal{K}_{\rm E1M1}$, $\mathcal{K}_{\rm E1CEDM2} < 0$, the curly brackets in (96) will take their largest value, 6.43 (CK model) and 3.53 (Cornell model). If we take $\mathcal{C}/\mathcal{A} < 0$ while $\mathcal{K}_{\rm E1M1}$, $\mathcal{K}_{\rm E1CEDM2} > 0$, the curly brackets will take their smallest value, 5.50 (CK model) and 3.08 (Cornell model). So the uncertainty of the values of the curly brackets caused by the uncertain signs of the SPA coefficients is 25% (CK model) and 13% (Cornell model). This is better than that obtained in Sec. IV. Note that the uncertainties in Sec. IV and V are caused by the uncertain signs of different terms.

Moreover, we may define another related observable. Define the asymmetry based on the CP-odd operator $\mathcal{O}$ as

$$A_{\mathcal{O}} \equiv \frac{N_{\rm events}(\mathcal{O} > 0) - N_{\rm events}(\mathcal{O} < 0)}{N_{\rm events}(\mathcal{O} > 0) + N_{\rm events}(\mathcal{O} < 0)}. \tag{97}$$

This may also be used to determine $\delta_c(d_c')$ experimentally.

So far there is no data on $\langle\mathcal{O}\rangle$. We expect BESIII to measure it.

IV. SUMMARY AND DISCUSSIONS

If the c-quark has an anomalous color-electric dipole moment (CEDM), it will serve as a new source of CP violation. In this paper, we study the determination of size $\delta_c(d_c')$ of the CEDM from the BESII data on the $M_{\pi\pi}$ distribution in $\psi' \to J/\psi\pi\pi$ within the framework of QCD.

We have first studied the contributions of the CEDM to the hadronic transition process $\psi' \to J/\psi\pi\pi$, and determined the size $\delta_c(d_c')$ of the CEDM by fitting the theoretical prediction to the BESII experimental data. The contributions are in two folds, namely, the contribution of CEDM to the $c\bar{c}$ interaction potential which causes CP-even and CP-odd states mixing, and the contribution of CEDM to the vertices in the hadronic transition which affect the $M_{\pi\pi}$ distribution in the transition. Both contributions lead to CP violation. Since CP violation is supposed to be small, we treat the CEDM effect as a perturbation throughout this paper. We studied these two kinds of contributions separately.

The perturbation calculations of the CEDM contribution to the $c\bar{c}$ potential and state mixings are given in Sec. II. The potential is the sum of the conventional potential V_0 and the CEDM contribution V_1. For V_0, we take two extreme QCD motivated potentials, namely, the CK potential and the Cornell potential to show the model dependence of the present approach. The expression for V_1 is shown in Eq. (6) in which only the second term contributes to state mixings. The obtained normalized state-mixing coefficients are given in Eq. (11) [see also (12)], and their numerical values are shown in Table I.

The CEDM contribution to hadronic transition vertices is more complicated. The 0th order transitions are shown in Eqs. (21) and (22) with $C_{10}^{10} = C_{20}^{20} = C_{12}^{12} = 1$. The $O(\delta_c^1)$ transitions are shown in Eqs. (23)–(28). The transition amplitudes of $O(\delta_c^1)$ transitions are proportional to δ_c, and their transition rates are proportional to δ_c^2. To the same order, we must also take account the transitions in (21) and (22) with the mixing coefficients of $O(\delta_c^2)$ in (78).

The calculation of the $M_{\pi\pi}$ distribution is quite subtle. A transition amplitude contains two factors, namely, the MGE factor and the hadronization (H) factor. For a given potential model, there is a systematic way of calculating the MGE factor [6,7]. The calculation of the H-factor is a highly nonperturbative problem in QCD. There are two approximation methods which can lead to the right order of magnitude of the transition rates [6,7,15,18], namely, the SPA and the 2GA. The SPA is a phenomenological approach which can correctly describe the angular relation between the two pions but it contains unknown constant coefficient(s) related to the hadronic matrix element in the H factor. The 2GA is a crude approximation which is easy to calculate but cannot describe the angular relation between the two pions correctly. Since we are dealing with the $M_{\pi\pi}$ distribution which concerns the angular relation between the two pions, we have to take the SPA. However, to our experience, the ratios between two transition rates in SPA and 2GA are quite close to each other [6,18]. Thus we can use this approximate relation and the 2GA calculation to express the $O(\delta_c^1)$ SPA coefficients in terms of the $O(\delta_c^0)$ SPA coefficients [cf. Eqs. (58), (66), and (76) in Sec. III]. Then we can predict the $M_{\pi\pi}$ distribution by treating the CEDM contribution as perturbation. The $O(\delta_c^0)$ and $O(\delta_c^2)$ contributions to the $M_{\pi\pi}$ distribution are given in Eqs. (34), (51), (61), (69), (70), (79), (83), and (85).

We then made a best fit of our 0th order prediction (34) to the BESII data (cf. Fig. 3), which determines the best fit values of the SPA parameters $|\mathcal{A}|$, $\mathcal{B}/\mathcal{A}$, and $|\mathcal{C}/\mathcal{A}|$ shown in Eq. (87). Various CEDM contributions to the $M_{\pi\pi}$ distribution are shown in Fig. 4. We see that the behaviors of the CEDM contributions are just the opposite to that of the 0th order contribution (cf. Fig. 3). This is why

the process $\psi' \to J/\psi\pi\pi$ can sensitively constrain $\delta_c(d_c')$. Next we included the CEDM contributions to make the best fit up to the $O(\delta_c^2)$. It is shown that, with the CEDM contribution, the fit is slightly improved (with slightly smaller χ^2), and the best fit values of $|\delta_c|$ and $|d_c'|$ are listed in Table IV. We see that the best fit value of $|\delta_c|(|d_c'|)$ is nonvanishing. However, considering the experimental errors, it is still consistent with zero. The 95% C.L. upper bound of $|d_c'|$ is shown in Eq. (88) which shows that the model dependence of the present approach is quite mild. Note that in the present approach, only the absolute values of the SPA coefficients in the CEDM contribution can be determined. So that each SPA coefficient still has an uncertain sign which may affect the result. This uncertainty is just due to the present phenomenological approach to the hadronization matrix element. We have discussed this uncertainty in Sec. IV, and the conclusion is that the uncertainty of the upper bound is (34–40)% which is not so serious. Thus, taking this theoretical uncertainty into account, we conclude that the 95% C.L. upper bound of $|d_c'|$ in the present approach is $|d_c'| < 3 \times 10^{-14}$ e cm [cf. Eq. (89)] which is the first experimentally determined upper bound of the CEDM of the c quark.

We have also proposed a second method for determining $\delta_c(d_c')$ linearly by introducing a CP-odd operator $\mathcal{O}$ and measuring its expectation value $\langle\mathcal{O}\rangle$ in Sec. V. We have shown in Sec. V that this is a better way of determining $\delta_c(d_c')$ experimentally. So far there is no such a measurement. We suggest BESIII to do this experiment.

The state mixings caused by the CEDM of the c quark makes the transition rates $\psi' \to h_c\pi^0$ and $\psi' \to J/\psi\pi^0$ related to each other. Hence, in principle, the experimental data of these two transition rates may give another constraint on d_c'. However, the latest BESIII sample of $\psi' \to h_c\pi^0$ based on 106 M of ψ' events is still rather small since the branching ratio of $\psi' \to h_c\pi^0$ is 8×10^{-4} [19], i.e., the statistical error in this transition rate is significantly larger than that in the present study. Furthermore, the transition $\psi' \to J/\psi\pi^0$ is dominated by E1M2 multipole gluon emissions, and the calculation of this kind of hadronization matrix element is not so certain [22]. Therefore the data of these two transition rates cannot provide a strong enough constraint on d_c' comparable to the one obtained in the present study. So far the best experiment for determining the bound on d_c' is $\psi' \to J/\psi\pi\pi$ at BES.

The BES detector has already been updated to BESIII with the efficiency of measuring low momentum pions significantly improved relative to BESII. So far BESIII has accumulated 1.06×10^8 ψ' events, and will be able to increase to $(7–10) \times 10^8$ ψ' events in 2012. That will be a huge sample. We expect that the new BESIII data may determine δ_c to a higher precision.

Estimating the CEDM from some UV theories may be interesting for future studies.

ACKNOWLEDGMENTS

We are grateful to Gang Li for providing us the original BESII data on $\psi' \to J/\psi\pi\pi$. We would like to thank Chien Yeah Seng for joining the early stage calculations in this study. This work is supported by National Natural Science Foundation under Grant Nos. 10635030, 10875064, 11135003, 10975169, and 11021092.

APPENDIX: CALCULATION OF THE MATRIX ELEMENT $_0\langle 1^1P_1|V_1|n^{(2s+1)}L_1\rangle_0$

We show here the explicit expression for the relevant matrix element $_0\langle 1^1P_1|V_1|n^{(2s+1)}L_1\rangle_0$. In the nonrelativistic limit, the state $|n^{(2s+1)}(L_i)_1\rangle_0$ can be decomposed into the radial, angular, and spin factors

$$\Phi_{nlmm_s}(r,\theta,\phi) = R_{nl}(r)Y_l^m(\theta,\phi)X_{m_s}^{(2s+1)}, \tag{A1}$$

where $R_{nl}(r)$ is the radial wave function obtained from solving the Schrödinger equation with a potential without V_1, and the spin state $X_{M_s}^{(2s+1)}$ is

$$\begin{aligned}
X_1^{(3)} &= \chi_{1/2}\bar{\chi}_{1/2} = \begin{pmatrix}1\\0\end{pmatrix}\begin{pmatrix}1\\0\end{pmatrix},\\
X_0^{(3)} &= \frac{1}{\sqrt{2}}[\chi_{1/2}\bar{\chi}_{-1/2} + \chi_{-1/2}\bar{\chi}_{1/2}]\\
&= \frac{1}{\sqrt{2}}\left[\begin{pmatrix}1\\0\end{pmatrix}\begin{pmatrix}0\\1\end{pmatrix} + \begin{pmatrix}0\\1\end{pmatrix}\begin{pmatrix}1\\0\end{pmatrix}\right],\\
X_{-1}^{(3)} &= \chi_{-1/2}\bar{\chi}_{-1/2} = \begin{pmatrix}0\\1\end{pmatrix}\begin{pmatrix}0\\1\end{pmatrix},\\
X^{(0)} &= \frac{1}{\sqrt{2}}[\chi - 1/2\bar{\chi}_{-1/2} - \chi_{-1/2}\bar{\chi}_{1/2}]\\
&= \frac{1}{\sqrt{2}}\left[\begin{pmatrix}1\\0\end{pmatrix}\begin{pmatrix}0\\1\end{pmatrix} - \begin{pmatrix}0\\1\end{pmatrix}\begin{pmatrix}1\\0\end{pmatrix}\right].
\end{aligned} \tag{A2}$$

There is a spin-dependent factor $(\boldsymbol{\sigma} - \bar{\boldsymbol{\sigma}}) \cdot \boldsymbol{r}/r$ in V_1. We can take the spherical coordinate

$$\begin{aligned}
&\frac{r_+}{r} \equiv \frac{1}{\sqrt{2}}\frac{x_1 + ix_2}{r} = -\sqrt{\frac{4\pi}{3}}Y_1^1(\theta,\phi),\\
&\frac{r_-}{r} \equiv \frac{1}{\sqrt{2}}\frac{x_1 - ix_2}{r} = \sqrt{\frac{4\pi}{3}}Y_1^{-1}(\theta,\phi),\\
&\frac{r_0}{r} \equiv \frac{x_3}{r} = \sqrt{\frac{4\pi}{3}}Y_1^0(\theta,\phi), \qquad \sigma_\pm \equiv \frac{1}{\sqrt{2}}(\sigma_1 \pm i\sigma_2),\\
&\bar{\sigma}_\pm \equiv \frac{1}{\sqrt{2}}(\bar{\sigma}_1 \pm i\bar{\sigma}_2), \qquad \sigma_0 \equiv \sigma_3 \qquad \bar{\sigma}_0 \equiv \bar{\sigma}_3\\
&\sigma_+(\bar{\sigma}_+) = \begin{pmatrix}0 & \sqrt{2}\\ 0 & 0\end{pmatrix}, \qquad \sigma_-(\bar{\sigma}_-) = \begin{pmatrix}0 & 0\\ \sqrt{2} & 0\end{pmatrix},\\
&\sigma_0(\bar{\sigma}_0) = \begin{pmatrix}1 & 0\\ 0 & -1\end{pmatrix},
\end{aligned} \tag{A3}$$

and express it as

$$(\boldsymbol{\sigma}-\bar{\boldsymbol{\sigma}})\cdot\frac{\boldsymbol{r}}{r}=(\sigma_0-\bar{\sigma}_0)\frac{r_0}{r}+(\sigma_+-\bar{\sigma}_+)\frac{r_-}{r}+(\sigma_--\bar{\sigma}_-)\frac{r_+}{r}$$
$$=\sqrt{\frac{4\pi}{3}}\{(\sigma_0-\bar{\sigma}_0)Y_1^0(\theta,\phi)+(\sigma_+-\bar{\sigma}_+)Y_1^{-1}(\theta,\phi)-(\sigma_--\bar{\sigma}_-)Y_1^1(\theta,\phi)\}. \quad \text{(A4)}$$

It is easy to see that

$$(\sigma-\bar{\sigma})_m X^3_{m_s}=2a_m(m_s)X^1,$$
$$a_m(m_s)=\left(-m_s\frac{1-m_s}{2},\,1-|m_s|,\,-m_s\frac{1+m_s}{2}\right),$$
$$m=+\qquad m=0\qquad m=-$$
$$(\sigma-\bar{\sigma})_m X^1=2a^*_m(m_s)X^3_{m_s},$$
$$a^*_m(m_s)=\left(-m_s\frac{1+m_s}{2},\,1-|m_s|,\,-m_s\frac{1-m_s}{2}\right),$$
$$m=+\qquad m=0\qquad m=- \quad \text{(A5)}$$

and $a_m(m_s)$, $a^*_m(m_s)$ satisfies

$$\sum_{mm_s}a_m(m_s)a_m(m_s)=3,\qquad \sum_{mm_s}a^*_m(m_s)a^*_m(m_s)=3,$$
$$\sum_{mm_s}a^*_m(m_s)a_m(m_s)=1. \quad \text{(A6)}$$

Thus

$$(\boldsymbol{\sigma}-\bar{\boldsymbol{\sigma}})\cdot\frac{\boldsymbol{r}}{r}X^3_{m_s}=\sqrt{\frac{4\pi}{3}}\{2a_0(m_s)Y_1^0(\theta,\phi)+2a_+(m_s)Y_1^{-1}(\theta,\phi)-2a_-(m_s)Y_1^1(\theta,\phi)\}X^1$$
$$(\boldsymbol{\sigma}-\bar{\boldsymbol{\sigma}})\cdot\frac{\boldsymbol{r}}{r}X^1=\sqrt{\frac{4\pi}{3}}\{2a^*_0(m_s)Y_1^0(\theta,\phi)+2a^*_+(m_s)Y_1^{-1}(\theta,\phi)-2a^*_-(m_s)Y_1^1(\theta,\phi)\}X^3_{m_s}. \quad \text{(A7)}$$

This explicitly shows that $(\boldsymbol{\sigma}-\bar{\boldsymbol{\sigma}})\cdot\boldsymbol{r}/r$ flips the quarkonium spin.

Next we evaluate the angular integration. What we need to evaluate is the integration of the product of 3 spherical harmonics. According to the property of the spherical harmonics, we have

$$\int Y^{m_f}_{l_f}(\theta,\phi)Y^m_1(\theta,\phi)Y^{-m_i}_{l_i}(\theta,\phi)d\Omega$$
$$=(-1)^{-m_i}\sqrt{\frac{3(2l_i+1)(2l_f+1)}{4\pi}}\begin{pmatrix}l_f & 1 & l_i\\ 0 & 0 & 0\end{pmatrix}\times\begin{pmatrix}l_f & 1 & l_i\\ m_f & m & -m_i\end{pmatrix}. \quad \text{(A8)}$$

The values of some relevant $3-j$ symbols are

$$\begin{pmatrix}1 & 1 & 0\\ m_f & m & 0\end{pmatrix}=(-1)^{1+m}\frac{\delta_{m_f,-m}}{\sqrt{3}},$$
$$\begin{pmatrix}1 & 1 & 2\\ 0 & 0 & 0\end{pmatrix}=\sqrt{\frac{2}{15}},$$
$$\begin{pmatrix}1 & 1 & 2\\ m_f & m & m_i\end{pmatrix}=(-1)^{m_f+m}\delta_{m_i,-m_f-m}\times\sqrt{\frac{(2+m_f+m)!(2-m_f-m)!}{30(1+m_f)!(1-m_f)!(1+m)!(1-m)!}}. \quad \text{(A9)}$$

Finally we evaluate the radial integration. There are two terms in $V_1(\boldsymbol{r})$ [cf. Eq. (6)]. We first look at the first term:

$$\frac{4}{3}\frac{\delta_c}{m_c}\int_0^\infty\frac{g_s(r)}{4\pi}R^*_{11}(r)\frac{\delta(r)}{r}R_{n_il_i}(r)r^2dr=\frac{8}{3}\frac{g_s(r)}{4\pi}\frac{\delta_c}{m_c}rR^*_{11}(r)R_{n_il_i}(r)|_{r=0}=0. \quad \text{(A10)}$$

Here we have considered the running of the QCD coupling constant $g_s(r)$ in the radial integration. Note that $g_s(r)$ is governed by asymptotic freedom as $r\to 0$, i.e. $g_s^2(r)\sim(1/\ln(\Lambda_{\overline{\rm MS}}r))$ as $r\to 0$ [cf. Eqs. (A14) and (A13) below]. Equation (A10) shows that the first term in Eq. (6) actually does not contribute. We should only take into account the contribution of the second term in Eq. (6) to the matrix element. The radial integration from the second term contribution is

$$-\frac{4}{3}\frac{\delta_c}{m_c}\int_0^\infty\frac{g_s(r)}{4\pi}R^*_{11}(r)R_{n_il_i}(r)dr=-\frac{4}{3}\frac{\delta_c}{m_c}I^{11}_{n_il_i},$$
$$I^{11}_{n_il_i}\equiv\int_0^\infty\frac{g_s(r)}{4\pi}R^*_{11}(r)R_{n_il_i}(r)dr. \quad \text{(A11)}$$

The radial wave function $R(r)$ is to be obtained by solving the Schrödinger equation.

To include nonperturbative contributions to $g_s(r)$ near the J/ψ and ψ' scales phenomenologically, we take the CK potential model which has both a clear QCD interpretation and successful phenomenological predictions. The CK potential reads [14]

$$V(r) = -\frac{16\pi}{25}\frac{1}{rf(r)}\left[1 + \frac{2\gamma_{\rm E} + \frac{53}{75}}{f(r)} - \frac{462}{625}\frac{\ln f(r)}{f(r)}\right] + kr, \tag{A12}$$

where $k = 0.1491\ \text{GeV}^2$ is the string tension related to the Regge slope, $\gamma_{\rm E}$ is the Euler constant, and $f(r)$ is

$$f(r) = \ln\left[\frac{1}{\Lambda_{\overline{\rm MS}} r} + 4.62 - \left(1 - \frac{1}{4}\frac{\Lambda_{\overline{\rm MS}}}{\Lambda^I_{\overline{\rm MS}}}\right) \times \frac{1 - \exp\{-[15(3\frac{\Lambda^I_{\overline{\rm MS}}}{\Lambda_{\overline{\rm MS}}} - 1)\Lambda_{\overline{\rm MS}} r]^2\}}{\Lambda_{\overline{\rm MS}} r}\right]^2, \tag{A13}$$

in which $\Lambda^I_{\overline{\rm MS}} = 180$ MeV. The nonperturbative effects resides in the phenomenological function $f(r)$. Writing the potential (A12) in the standard form $V(r) = -(4/3) \times [\alpha_s(r)/r] + kr$, we read from (A12) that

$$\alpha_s(r) \equiv \frac{g_s^2(r)}{4\pi} = \frac{12\pi}{25}\frac{1}{f(r)}\left[1 + \frac{2\gamma_{\rm E} + \frac{53}{75}}{f(r)} - \frac{462}{625}\frac{\ln f(r)}{f(r)}\right]. \tag{A14}$$

This running formula will be used in the calculation of $I^{11}_{n_i l_i}$ in (A11).

Putting all the above results together, we obtain the expressions for ${}_0\langle 1^1P_1|V_1|n_i{}^3S_1\rangle_0$ and ${}_0\langle 1^1P_1|V_1|1^3D_1\rangle_0$:

$${}_0\langle 1^1P_1|V_1|n_i{}^3S_1\rangle_0(m_f, m_s) = -\frac{8}{3\sqrt{3}}\frac{\delta_c}{m_c} I^{11}_{n_i 0}\delta_{m_f m_s}, \tag{A15a}$$

$${}_0\langle 1^1P_1|V_1|1^3D_1\rangle_0(m_f, m_i + m_s) = \frac{8}{3}\sqrt{\frac{2}{3}}\frac{\delta_c}{m_c} I^{11}_{12}\delta_{m_f, m_i + m_s}. \tag{A15b}$$

With these two matrix elements calculated, we can obtain all the mixing coefficients in (11) [cf. Eq. (12)].

For the spin-1 states. The conventional Cartesian coordinate representation of the spin = 1 operators are:

$$S_1 = \begin{pmatrix} 0 & 0 & 0 \\ 0 & 0 & -i \\ 0 & i & 0 \end{pmatrix}, \qquad S_2 = \begin{pmatrix} 0 & 0 & i \\ 0 & 0 & 0 \\ -i & 0 & 0 \end{pmatrix},$$
$$S_3 = \begin{pmatrix} 0 & -i & 0 \\ i & 0 & 0 \\ 0 & 0 & 0 \end{pmatrix}, \tag{A16}$$

i.e.,

$$(S_i)_{jk} = -i\epsilon_{ijk}. \tag{A17}$$

The eigenvectors of, for example, S_3 are:

$$\begin{matrix} m_s = +1 \\ \boldsymbol{\chi}_{1m_s} = \frac{1}{2}\begin{pmatrix} -(1+i) \\ 1 - i \\ 0 \end{pmatrix} \end{matrix} \qquad \begin{matrix} m_s = -1 \\ \boldsymbol{\chi}_{1m_s} = \frac{1}{2}\begin{pmatrix} 1 + i \\ 1 - i \\ 0 \end{pmatrix} \end{matrix} \qquad \begin{matrix} m_s = 0 \\ \boldsymbol{\chi}_{1m_s} = \frac{1}{2}\begin{pmatrix} 0 \\ 0 \\ 1 \end{pmatrix}, \end{matrix} \tag{A18}$$

where the column is ordered according to $i = 1, 2, 3$ from top to bottom. In the polar coordinate system, we should make the linear combination for the component index $(\chi_{1m_s})_{\pm 1} = [(\chi_{1m_s})_1 \pm i(\chi_{1m_s})_2]/\sqrt{2}$. Thus we obtain the following eigenvectors in the polar coordinate system:

$$\begin{matrix} m_s = +1 \\ \boldsymbol{\chi}_{1m_s} = \frac{1+i}{\sqrt{2}}\begin{pmatrix} 0 \\ 0 \\ -1 \end{pmatrix} \end{matrix} \qquad \begin{matrix} m_s = -1 \\ \boldsymbol{\chi}_{1m_s} = \frac{1+i}{\sqrt{2}}\begin{pmatrix} 0 \\ 1 \\ 0 \end{pmatrix} \end{matrix} \qquad \begin{matrix} m_s = 0 \\ \boldsymbol{\chi}_{1m_s} = \frac{1+i}{\sqrt{2}}\begin{pmatrix} 1 \\ 0 \\ 0 \end{pmatrix}, \end{matrix} \tag{A19}$$

where the column is ordered according to $m = +1, 0, -1$ top to bottom. Compared with Eq. (A5), we see that

$$(\chi_{1m_s})_m = \frac{1+i}{\sqrt{2}} a_m(m_s) \equiv N a_m(m_s), \tag{A19}$$

where $N \equiv (1+i)/\sqrt{2}$ is the normalization factor, and $N^*N = 1$.

Now the term $(\chi^*_{1m_{s2}})_j (S_i)_{jk} (\chi_{1m_{s3}})_k E_i$ in the E1-CEDM2 transition amplitude can be evaluated as

$$\begin{aligned} &(\chi^*_{1m_{s2}})_j (S_i)_{jk} (\chi_{1m_{s3}})_k E_i \\ &= -i\epsilon_{ijk}(\chi^*_{1m_{s2}})_j (\chi_{1m_{s3}})_k E_i \\ &= -i(\boldsymbol{\chi}^*_{1m_{s2}} \times \boldsymbol{\chi}_{1m_{s3}}) \cdot \boldsymbol{E} \\ &= \epsilon_{-m_1,-m_2,-m_3}(\chi^*_{1m_{s2}})_{m_2}(\chi_{1m_{s3}})_{m_3} E_{m_1} \\ &\overset{(A19)}{=} \epsilon_{-m_1,-m_2,-m_3} a_{m_2}(m_{s2}) a_{m_3}(m_{s3}) E_{m_1} \\ &= -i(\boldsymbol{a}(m_{s2}) \times \boldsymbol{a}(m_{s3})) \cdot \boldsymbol{E}. \end{aligned} \tag{A20}$$

[1] K. Nakamura *et al.* (Particle Data Group), J. Phys. G **37**, 075021 (2010).
[2] W. Bernreuther, U. Löw, J. P. Ma, and O. Nachtmann, Z. Phys. C **43**, 117 (1989).
[3] J. P. Ma, R. G. Ping, and B. S. Zou, Phys. Lett. B **580**, 163 (2004).
[4] T. M. Yan, Phys. Rev. D **22**, 1652 (1980).
[5] Y.-P. Kuang, Y.-P. Yi, and B. Fu, Phys. Rev. D **42**, 2300 (1990).
[6] Y.-P. Kuang and T.-M. Yan, Phys. Rev. D **24**, 2874 (1981).
[7] Y.-P. Kuang, Front. Phys. China **1**, 19 (2006).
[8] W. Bernreuther and O. Nachtmann, Phys. Lett. B **268**, 424 (1991).
[9] S. Weinberg, Phys. Rev. Lett. **63**, 2333 (1989); W. Buchmüller and D. Wyler, Nucl. Phys. **B268**, 621 (1986); J. Morozov, Sov. J. Nucl. Phys. **40**, 505 (1984).
[10] O. Nachtmann and C. Schwandenberger, Eur. Phys. J. C **13**, 315 (2000).
[11] D. Dicus, Phys. Rev. D **41**, 999 (1990); D. Chang, C.-S. Li, and T.-C. Yuan, Phys. Rev. D **42**, 867 (1990); A. Brandenburg, J.-P. Ma, R. Münch, and O. Nachtmann, Z. Phys. C **51**, 225 (1991).
[12] M. E. Peskin and D. V. Schroeder, *An Introduction to Quamtum Field Theory* (Addison-Wesley, Reading, MA, 1995), p. 125.
[13] E. Eichten, K. Gottfried, T. Kinoshita, K. D. Lane, and T.-M. Yan, Phys. Rev. D **17**, 3090 (1978); **21**, 203(E) (1980).
[14] Y.-Q. Chen and Y.-P. Kuang, Phys. Rev. D **46**, 1165 (1992).
[15] Y.-P. Kuang and T. M. Yan, Phys. Rev. D **41**, 155 (1990).
[16] Y.-P. Kuang, Phys. Rev. D **65**, 094024 (2002).
[17] L. S. Brown and R. N. Cahn, Phys. Rev. Lett. **35**, 1 (1975).
[18] Y.-P. Kuang, S. F. Tuan, and T.-M. Yan, Phys. Rev. D **37**, 1210 (1988).
[19] M. Ablikim *et al.* (BESIII Collaboration), Phys. Rev. Lett. **104**, 132002 (2010).
[20] D. Besson *et al.* (CLEO Collaboration), Phys. Rev. D **30**, 1433 (1984).
[21] M. Ablikim *et al.*, Phys. Lett. B **645**, 19 (2007).
[22] J. Z. Bai *et al.* (BESIII Collaboration), Phys. Rev. D **70**, 012006 (2004).